Alizé Deguette

The effects of a marine heatwave on seagrasses *Cymodocea nodosa* and *Zostera marina* in Ria Formosa, Portugal*:* photosynthetic activity & oxidative stress indicators

UNIVERSIDADE DO ALGARVE

Faculdade de Ciências e Tecnologia

2021

Alizé Deguette

The effects of a marine heatwave on seagrasses *Cymodocea nodosa* and *Zostera marina* in Ria Formosa, Portugal: photosynthetic activity & oxidative stress indicators

Mestrado em Biologia Marinha

Supervisor

Dr. João Miguel Sousa da Silva

Co-supervisor

Prof. Dra. Isabel Maria Alves Barrote

UNIVERSIDADE DO ALGARVE

Faculdade de Ciências e Tecnologia

2021

“The effects of a marine heatwave on seagrasses *Cymodocea nodosa* and *Zostera marina* in Ria Formosa, Portugal*:* photosynthetic activity & oxidative stress indicators”

Declaração de autoria de trabalho

Declaro ser a autora deste trabalho, que é original e inédito. Autores e trabalhos consultados estão devidamente citados no texto e constam da listagem de referências incluída.

Alizé Deguette

Aknowledgements

First, I would like to thank Dr. João Silva and Prof. Dra. Isabel Barrote, for giving me the opportunity to work on this project and for their friendly and kind help and attention all along this journey, in the field as well as in the laboratory. I sincerely had a good time learning and working with you both.

I would like to thank Diogo Paulo for his help during the seagrass collection and for teaching me some scuba-diving skills, the Ramalhete crew for their technical help during these two months of mesocosm experiment, and Monya Costa for her precious help in the laboratory. I learned a lot from you all.

Special thanks to Lorena Cojoc for her helping hand in the mesocosm maintenance.

Also, I would like to thank all my friends in Faro, coming from the four corners of the world, for making this whole master's experience so great.

Last but not least, thank you to my parents, who always encouraged me to pursue my dreams and gave me the keys to achieving my goals.

Thank you!

Abstract

Seagrasses play a high ecological role and provide a large range of ecosystem services, yet they are globally threatened by climate change. The seagrasses *Zostera marina* and *Cymodocea nodosa* share the same ecological niche in Ria Formosa, Southern Portugal, where their thermal distribution limits meet. While *C. nodosa* has its northern distribution limit in Portugal, *Z. marina* reaches its southern distribution limit in Ria Formosa. The present work aims to comparatively evaluate the physiological responses of both species to marine heatwaves (MHWs), a phenomenon that is increasing in frequency and intensity with climate change. Shoots of both species were transplanted into a mesocosm experiment where a MHW was simulated. The heatwave design was composed of a heating ramp from 20 to 28 °C, a 7-days heatwave at 28 °C, followed by a cooling ramp and an 8-days recovery period at 20 °C. The potentially stressful effects of the MHW on the plant's physiology were investigated, both during the MHW peak and after recovery. Photosynthetic performance was assessed with photosynthesis-irradiance (P-I) curves parameters (α, P_m and I_k) and chlorophyll fluorescence imaging (CFI). Complementarily, key biochemical stress indicators (Total phenols, TEAC, ORAC, MDA) were quantified to investigate the oxidative stress level in plant tissues. Only *C. nodosa* survived the acclimation period. The maximum quantum yield of photosystem II (Φ_{PSII}) was enhanced during the heatwave, probably to maintain the photosynthetic activity at control level. Negative effects on the photosynthetic performance of *C. nodosa* were observed after recovery, whereas Φ_{PSII} came back to control level**.** No significant oxidative stress was observed all along the experiment. Overall, although *C. nodosa* showed a relatively high tolerance to MHWs compared to other species such as *Z. marina*, *C. nodosa* population in Ria Formosa is likely to be negatively affected by the forecasted climate change scenarios.

Keywords

Marine heatwave, heat stress, chlorophyll fluorescence, Ria Formosa, *Zostera marina*, *Cymodocea nodosa*

Resumo

As pradarias de ervas marinhas estão entre os ecossistemas estuarinos e costeiros mais valiosos do ponto de vista ecológico. As ervas marinhas desempenham um papel ecológico importante e fornecem uma grande variedade de serviços ecossistémicos, como fonte de alimento, local de desova e berçário para várias espécies. Apesar de representarem apenas 0,1% da superfície do oceano, as pradarias de ervas marinhas são responsáveis por 20% sequestro global de "carbono azul". No entanto, a suas populações têm diminuído drasticamente (cerca de um terço desde a Segunda Guerra Mundial), principalmente devido ao aumento da pressão antropogénica e consequente aquecimento global. As ervas marinhas são altamente sensíveis às oscilações de temperatura. Aumentos de temperatura para valores acima do ótimo provocam-lhes stress e têm como consequências o decréscimo da performance fotossintética, o aumento da respiração, e perdas de biomassa, entre outras. As ondas de calor marinhas ou *Marine Heat Waves* (MHW), são caracterizadas por eventos com duração de pelo menos 5 dias, durante os quais a temperatura da água é superior ao limite relativo (geralmente o percentil 90) para um local e altura do ano específicos. Esses eventos, impulsionados principalmente pelas mudanças climáticas, têm-se tornado mais frequentes e intensos, ameaçando assim a sobrevivência de múltiplas espécies e o equilíbrio dos respetivos ecossistemas. Há, por isso, uma necessidade urgente de compreender a influência geral das MHW e, em particular, na fisiologia das ervas marinhas, tendo sempre em consideração as singularidades de cada espécie.

As ervas marinhas *Zostera marina* e *Cymodocea nodosa* partilham o mesmo nicho ecológico na lagoa costeira da Ria Formosa, no Sul de Portugal, onde se encontra o seu limite de distribuição. Enquanto a *C. nodosa* é uma espécie tropical de clima temperado e tem o seu limite de distribuição no Centro de Portugal, a *Z. marina* é uma espécie cosmopolita capaz de habitar uma vasta gama de perfis térmicos (desde temperados frios a subtropicais), atingindo o seu limite geográfico sul no sul de Portugal, nomeadamente na Ria Formosa. A Ria Formosa é um sistema mesotidal, onde a temperatura da água do mar geralmente varia entre 18 ºC e 30 ºC, entre Maio e Junho. No entanto, nos rasos de maré a fina coluna de água, acoplada à alta temperatura do ar e alta irradiância, provocam um aumento acentuado da temperatura da água que pode afetar significativamente a sobrevivência das ervas marinhas, especialmente, se associada às MHW. O presente trabalho teve como objetivo avaliar comparativamente as respostas fisiológicas de *Z. marina* e *C. nodosa* às MHW, para prever a evolução da sua distribuição espacial na Ria Formosa em cenários de alterações climáticas.

Unidades de ambas as espécies foram colhidas na lagoa Ria Formosa em Maio e imediatamente transplantadas, em cultura mista, para um sistema de mesocosmos onde permaneceram durante dois meses. Após 33 dias de aclimatação, foi simulada uma MHW, de acordo com a definição de MHW e com as características da área de estudo (climatologia local e limiar para esta época do ano). Para simular a MHW, a temperatura da água foi aquecida gradualmente de 20 ºC para 28 ºC. Seguiu-se um período de 7 dias a temperatura constante de 28 ºC (MHW). Procedeu-se depois ao arrefecimento gradual da água até aos 20 ºC, temperatura que se manteve durante 8 dias (período de recuperação). Para investigar o efeito da MHW e se há consequências após o alívio da temperatura, foram amostradas folhas maduras no fim da MHW e no fim do período de recuperação. O desempenho fotossintético das plantas foi estimado através de curvas fotossintéticas de resposta à luz (curvas P-I) e respetivos parâmetros: eficiência fotossintética (α), taxa fotossintética máxima (P_m) e irradiância de meia saturação (I_k) usando o modelo Jassby & Platt (1976).

A análise da imagem da fluorescência da clorofila *a* (CFI) foi usada para medir o rendimento quântico efetivo do fotossistema II (Φ_{PSII}). As CFI permitiram identificar e comparar as respostas entre as idades do tecido foliar (velho, maduro e jovem) das ervas marinhas. Os principais indicadores bioquímicos de stress (fenóis totais, TEAC, ORAC e MDA) foram também quantificados para investigar os efeitos das MHW sobre a atividade antioxidante e o potencial dano oxidativo nos tecidos foliares. A razão área *vs* peso seco (ou *dry weight*, DW) das folhas foi investigada para avaliar as mudanças na biomassa das folhas.

Apenas a *C. nodosa* sobreviveu ao período de aclimatação. A atividade fotossintética das folhas de *C. nodosa* em resposta à intensidade luminosa apresentou a forma hiperbólica típica. Embora o desempenho fotossintético de *C. nodosa* se tenha alterado durante a onda de calor (aumento de Φ_{PSII}), foram observados efeitos negativos em α, P_m e I_k (2 a 4 vezes menor) após a fase de recuperação. O aumento de Φ_{PSII} durante a onda de calor, pressupõe o aumento no transporte de eletrões o qual terá permitido manter α, P_m e I_k inalterados. Não obstante, Φ_{PSII} de *C. nodosa* voltou ao nível de controlo após o período de recuperação. Considerando a idade dos tecidos foliares, o valor de Φ_{PSII} foi maior nas zonas maduras do que nas zonas velhas, especialmente durante a onda de calor. Este resultado é corroborado pela CFI. Não foi observado efeito significativo da MHW na atividade antioxidante nem ocorreram danos oxidativos significativos nas folhas de *C. nodosa*, sugerindo que o sistema antioxidante das folhas de *C. nodosa* foi suficiente para evitar o stress oxidativo. No entanto, verificou-se uma tendência para o aumento da concentração de todos os indicadores bioquímicos de stress

oxidativo após a recuperação da onda de calor, embora não de forma significativa. Esta tendência poderá indicar que uma MHW mais longa e/ou mais intensa poderá implicar o aumento significativo do stress oxidativo e o dano celular nas folhas de *C. nodosa*, com repercussões a longo prazo na sua fisiologia. Observou-se também que a simulação da MHW provocou o aumento da razão área *vs* DW, especialmente após a recuperação. Este resultado pode estar relacionado com a redução da taxa de crescimento e espessura foliar de *C. nodosa*, ou com um possível aumento no volume do aerênquima (canais de ar no interior das folhas), que melhoraria a difusão dos gases, nomeadamente O_2, no interior das folhas sob stress térmico. Em suma, os nossos resultados sugerem que embora as plantas de *C. nodosa* da Ria Formosa apresentem alguma tolerância e plasticidade fisiológica a este tipo de MHW, é provável que sofram as consequências de tais eventos a longo prazo. Mesmo que as temperaturas ótimas de *C. nodosa* sejam mais altas do que as de outras espécies de ervas marinhas no mesmo ambiente térmico, como *Z. marina*, uma MHW como a de 28 °C usada no presente trabalho, poderá impactar negativamente a população de *C. nodosa* na Ria Formosa. Deste modo, sugerimos que os efeitos das MHW podem ter consequências mais dramáticas na biologia de *C. nodosa* se ocorrerem durante uma época do ano em que as temperaturas sazonais são mais baixas, ou se forem mais frequentes, intensas e duradouras, conforme o previsto pelo cenário das mudanças climáticas. Assim, através do exemplo da Ria Formosa, este estudo destaca a importância da continuação do desenvolvimento de estudos sobre a fisiologia das ervas marinhas para a sua conservação em todo o mundo.

Atendendo às características dos parâmetros relacionados com as MHW (temperatura, duração, época do ano...), o estudo dos seus efeitos nas pradarias marinhas deve ser aprofundado, e incluir os seus efeitos acoplados (duração e intensidade) a longo prazo, e em diferentes épocas do ano.

Table of contents

List of figures

Introduction

Materials and methods

Results

List of tables

Materials and methods

Results

Abbreviations list

ABAP – 2,2-azobis(2-amidinopropane) hydrochloride

ABTS$^{\bullet+}$ – 2,2′-azinobis (3- ethylbenzothiazoline-6-sulphonic acid)

AOI – Area of interest

C – Control

c – Curvature parameter

CFI – Chlorophyll fluorescence imaging

DR – Dark respiration

DW – Dry weight

ETR – Electron transfer rate

F'_m – Maximum fluorescence of the light-adapted leaf tissue

F_s – Steady-state fluorescence of the light-adapted leaf tissue

FW – Fresh weight

GP – Gross photosynthesis

HAT – Hydrogen atom transfer

HSP – Heat stress protein

HW – Heatwave

I – Irradiance

I_k – Half-saturation irradiance

MDA – Malondialdehyde

MHW – Marine heatwave

NP – Net photosynthesis

ORAC – Oxygen radical absorbance capacity

PAR – Photosynthetically available radiation

P-I – Photosynthesis-Irradiance

P_m – Maximum photosynthetic rate

PSI – Photosystem I

PSII – Photosystem II

R – Recovery

RF – Ria Formosa

ROS – Reactive oxygen species

SST – Sea surface temperature

TBA – Thiobarbituric acid

TEAC – Trolox equivalent antioxidant capacity

T_{max} – Maximum temperature

TPC – Total phenolic compounds

α – Photosynthetic efficiency

Φ_{PSII} – Effective quantum yield of photosystem II

1. Introduction

1.1. Marine heatwaves, an intensifying phenomenon

In the context of climate change and global warming, heatwaves are often pointed out as yet another negative consequence of those processes. Well-known to happen above the sea level, they also occur in the marine environment and are characterized by an abnormal increase in water temperature. Only recently, and pressured by the urgency of the climatic threat, the scientific community started qualifying and understanding the marine heatwave (MHW) phenomenon. The Intergovernmental Panel on Climate Change (IPCC) defined MHW as "an event at a particular place and time of the year that is rare and predominately, but not exclusively, defined by a relative threshold; that is, an event rarer than 90th or 99th percentile of a probability density function", in the Special Report on the Ocean and Cryosphere (SROCC, 2019). Although global warming has been proved to be the primary driver of MHWs (Perkins-Kirkpatrick et al., 2019), it is not the only one: many physical drivers, such as the intensification of marine currents, changes in atmospheric pressure, El Niño/La Niña events, coupled air-sea interactions, etc. also take part in the emergence of MHWs (Holbrook et al., 2019; Holbrook et al., 2020). MHW can occur at any time of the year (not only in summer), everywhere in the world, for a period ranging from a few days to several weeks at varying intensities. They have severely increased in frequency and intensity in the past century (Figure 1.1; +54% increase in annual MHW days globally; Oliver et al., 2018), as an unstoppable cause of massive extinctions ("The Blob", a large mass of water in the Pacific Ocean which temperature was high above normal, killed nearly a million seabirds in Alaska and California in 2015-2016; Gibble et al., 2018), range shifts (Brodeur et al., 2019) and coral bleaching (mass coral mortality occurred in the Great Barrier Reef in 2016, with losses exceeding 50%; Le Nohaïc et al., 2017; Hughes et al., 2018; Genevier et al., 2019; Leggat et al., 2019).

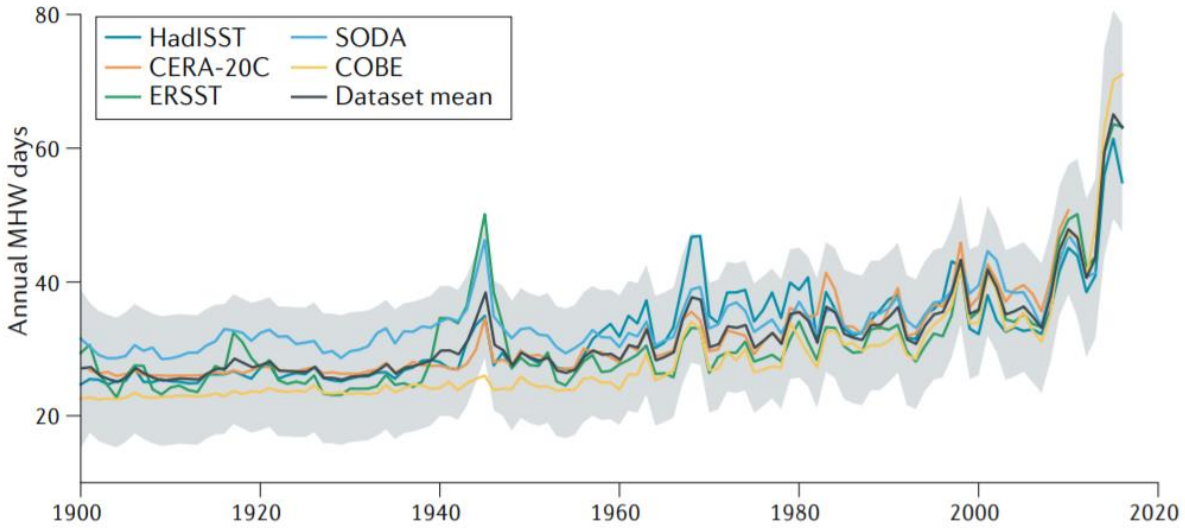

Figure 1.1: Globally averaged changes in the annual number of MHW days based on the Hadley Centre Sea Ice and Sea Surface Temperature (HadISST)119, Extended Reconstructed Sea Surface Temperature (ERSST)120, COBE121, CERA-20C122 and Simple Ocean Data Assimilation (SODA) datasets. Grey shading indicates the 95% confidence interval. (In Holbrook et al., 2020)

The consequences of MHWs can also be dramatic on human health (Guirguis et al., 2014), fisheries, aquaculture, biodiversity conservation (from plankton to algae and marine mammals; Cunha et al., 2014; Brodeur et al., 2019) and on a variety of ecosystem services (Smale et al., 2019). Projections are pessimistic about what is yet to come and predict an increase in MHWs frequency and intensity, as a direct cause of the increasing anthropogenic global warming (Oliver et al., 2019). In the last decade, intensive research efforts have been undertaken to understand this phenomenon and raise awareness about its effects (Figure 1.2; Hobday et al., 2018). The Marine Heatwaves international working group, initiated in May 2014, gathers information and research articles online about the topic, making it accessible and understandable to everyone (http://www.marineheatwaves.org). Knowledge and prediction of MHWs are more than ever required to allow to adapt our activities to ensure the sustainability of our resources and maintain biodiversity.

As is the case worldwide, MHWs also occur along the Portuguese coast, changing the environmental conditions of fragile ecosystems, such as seagrass meadows.

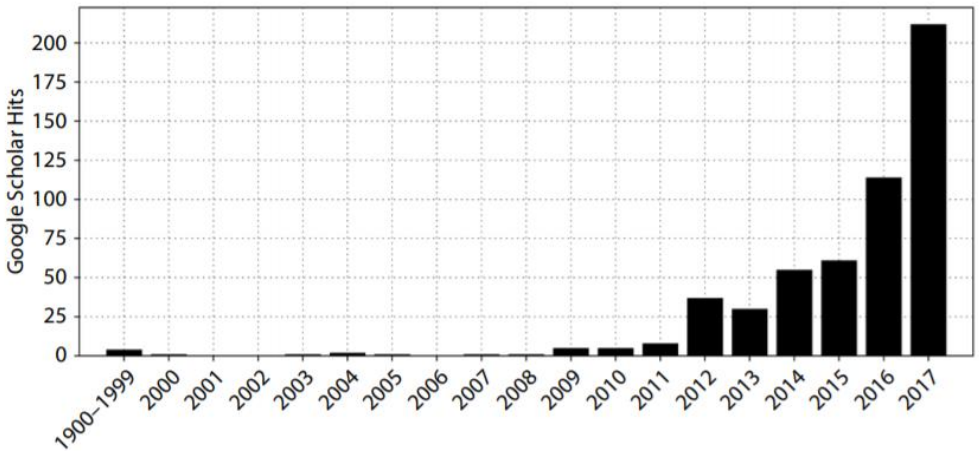

Figure 1.2: Frequency of publications returned from a Google Scholar search based on the search terms "marine heatwave" and "marine heat wave." Note that the first bin (1999) contains all records for the period 1900–1999. (In Hobday et al., 2018)

1.2. Seagrasses: key elements in marine ecosystems

Seagrasses are angiosperms (flowering plants) adapted to marine life, accounting for about 60 species worldwide (Green & Short, 2003). They are clonal plants, which shoots grow from the expansion of rhizomes (Duarte, 2002). They are found worldwide along tropical, temperate and boreal latitudes, except in the Antarctic region, colonizing intertidal areas and shallow waters in subtidal zones (Figure 1.3; Alongi, 2018).

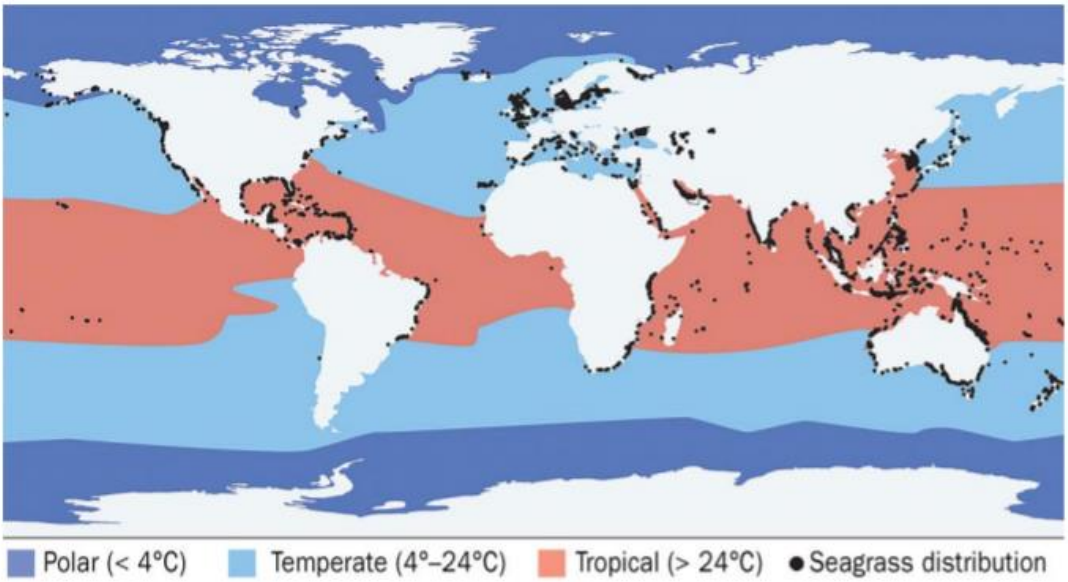

Figure 1.3: Global distribution of seagrass meadows in relation to mean ocean temperature. Regional divisions are based on polar (< 4°C), temperate (4°C-24°C) and tropical (> 24°C) climate. (In Green & Short, 2003)

Seagrass meadows are among the most ecologically valuable estuarine and coastal ecosystems, as they provide many essential ecosystem services. Notably, they slow down the currents, trap suspended particles and, in this way, increase light penetration (Carr et al., 2010). They offer valuable feeding, spawning and nursery grounds for numerous species (Blandon and Zu Ermgassen, 2014) of flora and fauna and they enhance the production and biodiversity of adjacent ecosystems (Boudouresque et al., 2006). Seagrasses have been more and more studied because of their role as carbon sinks (Duarte et al., 2010; Cabaço and Santos, 2014; Marbà et al., 2018, Bañolas et al., 2020), which has major importance in "blue carbon" sequestration and export (Duarte and Krause-Jensen, 2017). Although they represent less than 0.1% of the ocean surface, seagrasses are responsible for 20% of carbon sequestration globally (Duarte et al., 2005; Kennedy et al., 2010). Regrettably, seagrass meadows are declining globally at a dramatic rate (110 km^2 $year^{-1}$ since 1980 i.e., 5% $year^{-1}$ globally or at least 1/3 since World-War II; Orth et al., 2006; Waycott et al., 2009) because of the environmental changes they are facing. Notably, MHWs have been proved to be one of the major drivers of seagrass decline (36% of Shark Bay's - Western Australia - seagrass meadows were negatively affected by a MHW in 2010/11; Arias-Ortiz et al., 2018). In fact, a temperature increase above the optimum temperature of seagrasses reduces the photosynthetic rate and leave's productivity, and increases respiration, photosynthetic stress responses and biomass losses (Collier et al., 2017; George et al. 2018). In addition, the effects are even more considerable as the number of thermal stress days increases, with species-specific responses (George et al. 2018; Savva et al., 2018).

In Europe, 35 684 ha of seagrass meadows disappeared between 1869 and 2016, i.e., 29% of the area documented by de los Santos et al. (2019). The same study showed that the highest proportions of declines were reported for the species *Zostera marina* and *Cymodocea nodosa* (net losses of 57% and 46% of the documented area, respectively). Despite the general decline of seagrasses in Europe between 1869 and 2016, gain was reported in the 2000s, for the first time since the 1950s (20% net gain in area per decade in the 2000s; de los Santos et al., 2019), showing a significant trend reversal as a result of conservation and restoration actions. Thus, seagrass decline is neither irreversible nor to be generalized: hope remains to maintain or even improve the services they provide.

1.3. *Cymodocea nodosa* and *Zostera marina*, two co-occurring species in Ria Formosa

Ria Formosa is populated with three seagrass species: *Zostera noltii* in the intertidal and *Zostera marina and Cymodocea nodosa* in the subtidal (Cabaço and Santos, 2010; Cabaço et al., 2010; Guimarães et al., 2012). Both *Z. marina and C. nodosa* share the same ecological niche in the lagoon, where they are found in mixed patches.

Z. marina (or eelgrass) is the scarcest of the three seagrass species found in Ria Formosa (followed by *C. nodosa*), where it reaches its southern distribution limit (Cabaço and Santos, 2010). It is the most endangered seagrass species in Portugal (Cunha et al., 2014) and is now found at only a few locations in the country: Lagoa de Óbidos, Ria Formosa (Cabaço and Santos, 2010), where was reported to cover an area of 0.05 km² in 2007 (Cunha et al., 2014), and more recently in the Ria de Aveiro lagoon (Guerrero-Meseguer et al., 2021). In the Ria Formosa lagoon, Massa et al. (2009) and Cunha et al. (2014) reported local extinctions of the seagrass *Z. marina*, which were correlated to above-climatology summer temperatures.

The European *Z. marina* is generally used in heat shock or heatwave experiments as it is a cosmopolitan species, distributed in a wide range of thermal environments (from temperate to subtropical waters) along the coasts of the Northern Hemisphere (Green & Short, 2003). Having populations from such different environments allows us to compare the responses and adaptations of the plant to thermal stress (Winters et al., 2011), which differences may be significant under climate change scenarios. Previous studies (Bergmann et al., 2010; Franssen et al., 2014) suggested that *Z. marina* would tend to disappear from its southern range as heat shocks have negative impacts on its metabolism. In addition, above-normal sea surface temperature (SST) has been proved to negatively impact the flowering and reproductive intensity of *Z. marina* (Qin et al., 2020). Gao et al. (2019) investigated the physiological responses of eelgrass shoots to a 48-h incubation at 32 °C, which resulted in important shifts in physiological stress indicators: inhibition of photosynthetic efficiency (-23.9%), increased respiration (+58.3%), and decreased carbohydrate decomposition products, showing an energy supply decrease and a membrane deficiency caused by high temperatures. These studies (not exhaustively) show the ability of *Z. marina* to regulate its metabolism and/or modulate its membrane functionality according to water temperature and tend to show that high temperatures negatively impact its biology. Although the bibliography is relatively dense about *Z. marina*, research is scarcer about *C. nodosa*.

C. nodosa (Ucria) is a temperate-warm adapted species, resistant to relatively high water temperatures (25–32 °C; Olsen et al., 2012; Marín-Guirao et al., 2016). As a tropical-originated species, *C. nodosa* has a high optimum temperature range (24.5 and 31.0 ± 0.5 °C for growth and photosynthesis, respectively) comparing to temperate species in the Mediterranean, such as *Z. marina* (15.3 ± 1.6 and 23.3 ± 1.8 °C, respectively; Lee et al., 2007). Its distribution ranges from its northern limit on the southern Portuguese coast (Cunha et al., 2014) to its southern limit in Senegal (Lüning, 1990). In 2007, *C. nodosa* was reported to cover an area of 0.913 km² in Ria Formosa, accounting for the second most abundant seagrass in the lagoon after *Z. noltii* (Cunha et al., 2014). The evolution of *C. nodosa* between 1998 and 2008 in Ria Formosa was studied by Cabaço and Santos (2014), showing that in one decade, *C. nodosa* populations declined dramatically in this area, although the nutrient supply allows high growth and production rates to this nutrient-limited species (Falcão and Vale, 1990; Perez et al., 1994). Cabaço and Santos (2014) reported that in one decade, two of the four meadows initially present disappeared due to sediment erosion and burial, both related to the anthropic pressure of coastal engineering and/or eutrophication (Cunha & Duarte, 2005).
While the effects of heatwaves and heat shocks were mainly studied for *Z. noltii* and *Z. marina* (Massa et al., 2009; Franssen et al., 2011; Winters et al., 2011; Franssen et al., 2014; Repolho et al., 2017; Gao et al., 2019), to our knowledge only one paper was published about the effect of heatwaves upon *C. nodosa* (Marín-Guirao et al., 2018). This study underlined the effect of a simulated MHW on *C. nodosa* shoots coming from different thermal environments, showing that the species could recover from the MHW, with differences between shoots coming from warm and cold waters (thermal adaptation).

1.4. Main objectives

The main objective of this work was to comparatively investigate the tolerance and physiological plasticity of *C. nodosa* and *Z. marina* in coping with MHWs, in order to understand how near to thermal tolerance both species are in Ria Formosa. However, for unknown reasons, most *Z. marina* shoots did not survive the transplant to the experimental facility, and therefore only the results for *C. nodosa* will be presented and discussed.

Specific objectives of the present work are:

- To investigate the effect of a MHW in the short and long term on the photosynthetic performance of different tissue ages.
- To quantify the biochemical oxidative-stress indicators and evaluate the impact of an MHW on the leaves' antioxidant activity and potential oxidative damage.
- To assess the effect of a MHW on the leaves' biomass.

This work will help understand and forecast *C. nodosa*'s tolerance and future spatial distribution under climate change scenarios that include more frequent and intense MHWs.

2. Materials and methods

2.1. Study site

The Ria Formosa coastal lagoon, located in the south coast of Portugal (36°58'N, 8°02'W to 37°03'N, 7°32'W), is an 84 km² shallow mesotidal lagoon. It has been a Natural Park since 1987 and is a Ramsar and Natura 2000 protected area. It is one of the most important wetlands in Europe, spanning over 55 km long and a maximum of 6 km width (Newton & Mudge, 2003). The lagoon is 2 m deep on average and its tidal amplitude varies between 3.50 m on spring tides and 1.30 m on neap tides (Instituto Hidrográfico, 1986). It is separated from the Atlantic Ocean by five dynamic barrier islands and two peninsulas and is linked to it by seven channels, five natural and two artificial, allowing water exchange with the ocean. Essentially composed of salt marshes and mudflats in the intertidal and shallow channels in the subtidal, the highly productive Ria Formosa hosts a rich diversity of fauna and flora. It is an important nursery hotspot and feeding ground for many fishes and molluscs (Andrade, 1985), which gives the lagoon high ecological importance. The mean air temperature is 25°C in summer and 12°C in winter, which gives Ria Formosa a Mediterranean climate, despite being situated on the Atlantic coast (Newton & Mudge, 2003). In this mesotidal system, May-June seawater temperature commonly ranges between 18 °C and 30 °C (https://www.hidrografico.pt/boias). However, in intertidal pools and shallow subtidal areas, the thin water column (especially during low spring tides), coupled to high air temperature and high irradiance, drives the water temperature to rise dramatically, especially in summer (Massa et al., 2009) when it can reach 35°C (João Silva, personal communication). Such

drastic environmental changes can significantly affect the physiology and survival of all types of species found in the Ria Formosa, including seagrasses.

2.2. Experimental design

2.2.1. Plant collection

C. nodosa and *Z. marina* plants, including rhizomes, roots, apical meristem, and shoots with 3-4 leaves each, were carefully collected in Ria Formosa's main channel and in Ramalhete channel on May 3rd, 2021 (Figure 2.1). In total, approximately 300 shoots were collected per species.

Figure 2.1: Satellite view of the Ria Formosa lagoon in Faro and Olhão area, on the South coast of Portugal. *C. nodosa* and *Z. marina* sampling sites (S1 and S2, respectively) are marked with red dots (Google satellite, WGS84).

Following collection, shoots were submerged in seawater in closed dark tanks (Figure 2.2) and immediately transferred to Ramalhete experimental station. Dark tanks were aerated until transplantation into the mesocosm facility, within 24 h of uprooting.

Figure 2.2: Pictures taken during the plants collection on May 3rd, 2021. *Z. marina* shoots collection, approximately 3m deep (a) and uprooted *Z. marina* shoots inside the dark tanks, waiting for the transplant (b).

2.2.2. Experimental setup: a common garden mesocosm experiment

An indoor mesocosm experiment ("common garden" design) was conducted in Ramalhete station. Ten 65-L plastic tanks (5 replicates per treatment, n=5) were filled with 15 cm of sand collected from Faro beach and supplied with water pumped from Ria Formosa through an open circuit. To reduce microalgae development and contamination in the facility, water pumped from Ria Formosa was flowing through a 50-W UV filter before entering the circuit. The water temperature in the circuit was controlled with a temperature controller (ECLI20MA IKOMFORTRC900 inverter, i-Komfort, Kripsol, Toledo, Spain) and flowed in the aquaria at a rate of 14 L h^{-1} so that the water was entirely renewed every 5 h. The aquaria were aerated with a bubbling air pipe, and water was kept in motion and homogenised with a water fan. The light above each tank was provided by LED lamps (Ledvance Flood LED 50W/6500K WT, Augsburg, Germany) hung above each tank in such a way as to provide approximately the same light intensity in the spectral range from 400 to 700 nm to each aquarium. Light intensity in this spectral range was measured and calibrated before starting the experiment with a LI-250A Light Meter and a LI-190R sensor (LiCor, USA) and ranged from 101.6 to 130.8 µmol m^2 s^{-1} (113.2 µmol m^2 s^{-1} on average) just on top of the water surface. To simulate the natural conditions, the lights were automatically turned on at 6 a.m. and off at 9 p.m. (photoperiod of 15 h:9 h).

The day following harvesting, seagrass shoots were carefully cleaned from epiphytes and placed in the aquaria under controlled conditions of light and temperature. Approximately 25 shoots of *C. nodosa* and 25 shoots of *Z. marina* were planted in each aquarium (mixed culture; Figure 2.3).

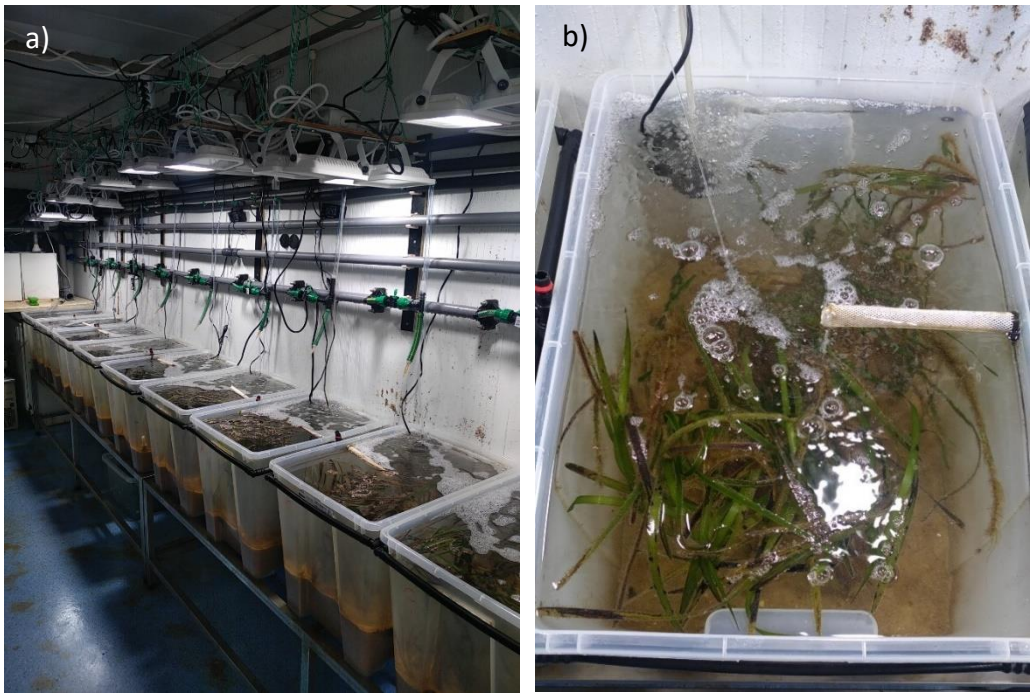

Figure 2.3: Pictures of the experimental setup (a) and a view from the top of one aquarium during acclimation (b), with a mixed *C. nodosa* and *Z. marina* culture.

The two treatments (Control, C and Heatwave, HW) were randomly assigned to the aquaria (Figure 2.4). Following the transplant, shoots were left 33 days at 20 °C (1 °C above the water temperature during collection) to allow the plant to acclimate to their new environment. While the C aquaria were kept at 20 °C all along the experiment, the MHW simulation was applied in the HW aquaria. Throughout the acclimation and experimental periods (detailed below), temperature was daily monitored in all tanks, at the warmest time of the day (between 2 and 4 p.m.), with a manual thermometer. In addition, 5 HOBO temperature loggers were randomly placed in tanks for continuous temperature records. During the heatwave simulation (heating ramp, heatwave peak and cooling ramp), the temperature was monitored and controlled in each of the five HW tanks with a temperature controller (AquaMedic T controller twin, Bissendorf, Germany).

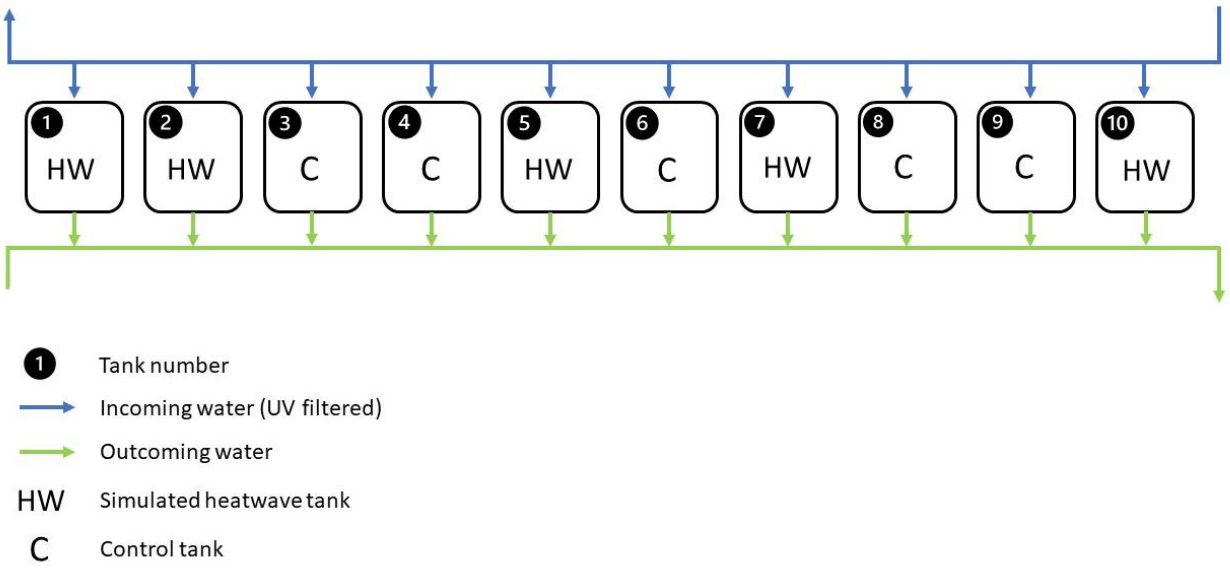

Figure 2.4: Scheme of the experimental setup with tank number, random treatment assignation (Control, C and Heatwave, HW) and water flow direction (open circuit).

2.2.3. Heatwave characteristics

Determination of the maximum temperature (T_{max}) of the simulated heatwave was based on previous *in situ* temperature records. To get a proxy of the yearly temperature in *Z. marina* and *C. nodosa* beds in Ria Fomosa, temperature data previously recorded in both water and sediment of *Caulerpa prolifera* beds (mean daily temperature data, from 10-06-2017 to 17-06-2019; de los Santos, personal communitcation) were used. *C. prolifera* is found at a similar depth to *Z. marina* and *C. nodosa*'s natural conditions (Cunha et al., 2013). As the water and sediment temperature data were similar (Figure 2.5), both were used to form a single dataset, as a proxy for temperature in *Z. marina* and *C. nodosa* beds.

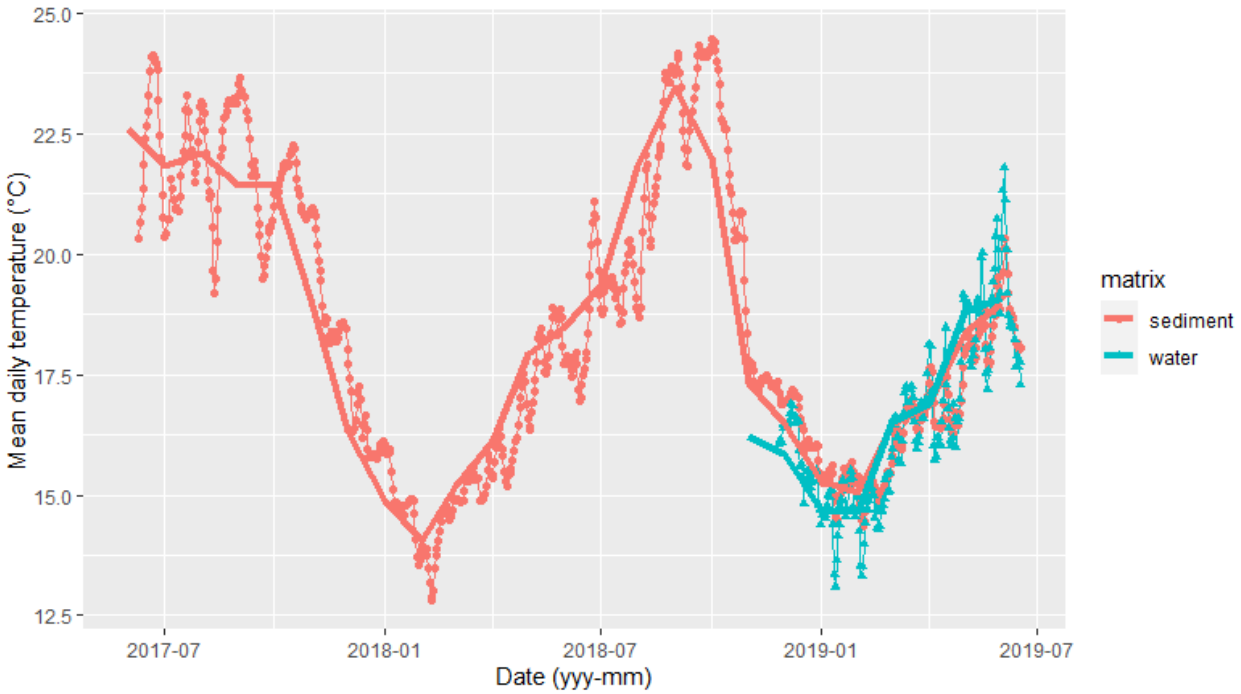

Figure 2.5: Mean daily temperature over time in *C. prolifera* beds in Ria Formosa, in the overlying water and sediment, used as a proxy for temperature in *Z. marina* and *C. nodosa* beds. Time ranges from 10-06-2017 to 17-06-2019 (approximately two years) for both datasets together.

To determine if heatwave events occur during this time range, the NOAA Optimum Interpolation Sea Surface Temperature (OISST) dataset (Huang et al., 2020; methodology developed by Reynolds et al., 2007 and described by Benzon et al., 2016) was analysed. This daily temperature dataset, displayed on the Marine Heatwaves Tracker app (Schlegel, 2020), contains the oceanic SST, climatology (Hobday et al., 2016), threshold ("90th percentile relative to the local long-term climatology", Hobday et al., 2016) data and the heatwave events record from 1982 to the present day. A pixel close to Ria Formosa's inlet channel (Lon = 7.875°W, Lat = 36.875°N) was selected and a time series was plotted for the 10-06-2017 to 17-06-2019 time range (Figure 2.6).

Figure 2.6: Time series of oceanic water SST adjacent to Ria Formosa, from 10-06-2017 to 17-06-2019 (black line). Blue scattered line: climatology; red dotted line: threshold; orange-coloured: marine heatwave; red-coloured: heatwave peak. Red marks on the x-axis indicate MHWs events. (Adapted from the Marine Heatwave Tracker app; Schlegel, 2020)

To determine the temperature inside Ria Formosa during a heatwave event, and the potential difference to oceanic MHWs, the correlation between the temperature inside and outside Ria Formosa was established for the year 2018 (Figure 2.7).

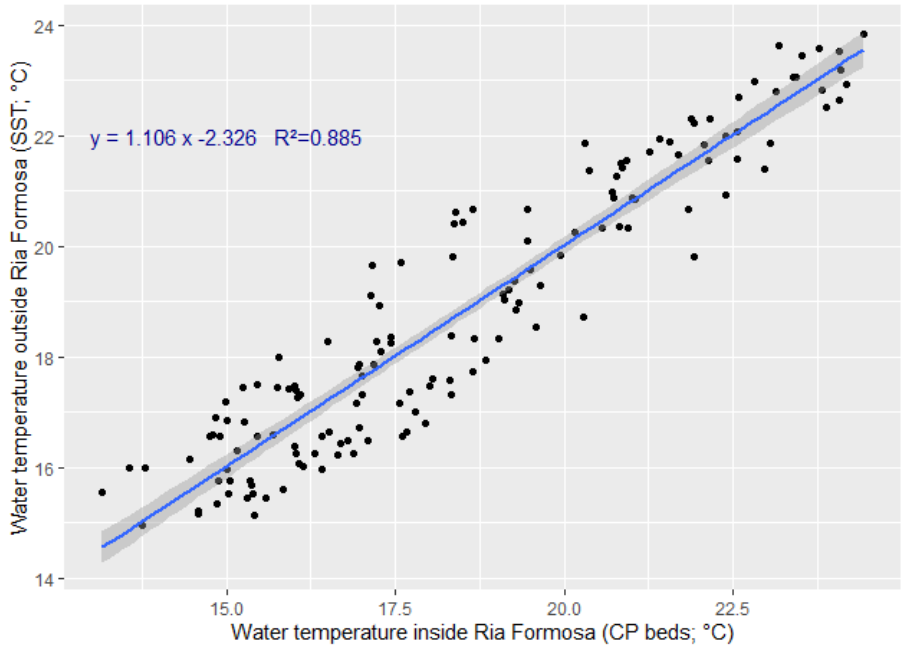

Figure 2.7: Linear regression plot assessing the correlation between the water temperature inside and outside Ria Formosa (SST, data recorded by an oceanographic buoy of the Instituto Hidrográfico) in 2018, and corresponding correlation equation. Data frequency is every five days.

Using the observed high correlation between the two datasets (R^2=0.885), the SST climatology line inside Ria Formosa was then extrapolated (Figure 2.8).

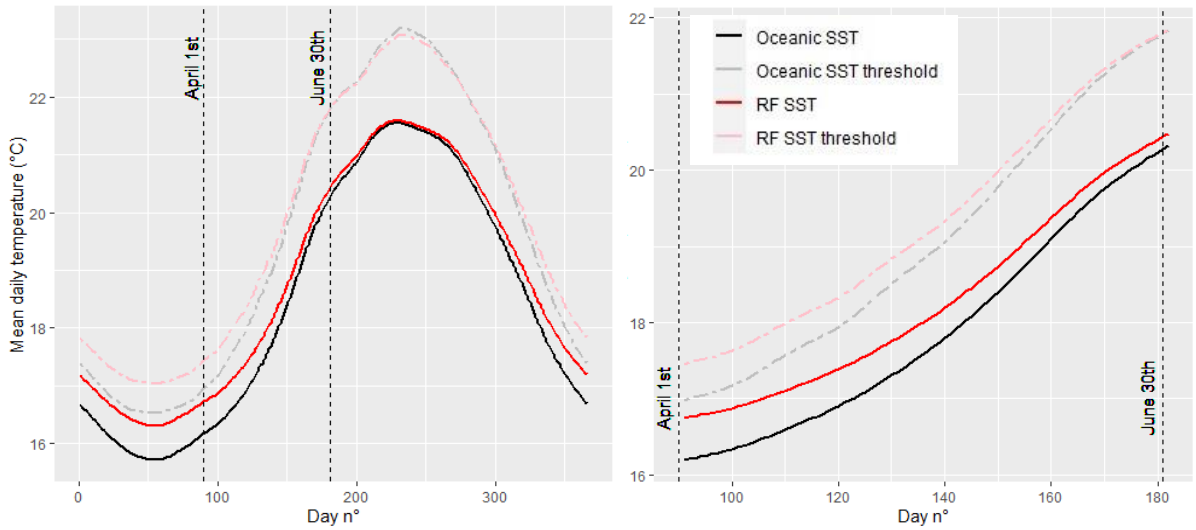

Figure 2.8: Oceanic SST climatology (from NOAA OISST) and threshold, and extrapolated Ria Formosa's (RF) SST climatology and threshold for the year 2018 (left) and for April 1st to June 30th (right), according to the correlation equation y= 1.106x -2.326.

The occurrence of MHWs close to Ria Formosa for this time of the year was prospected in the historic data available at the Marine Heatwaves Tracker website (Figure 2.9).

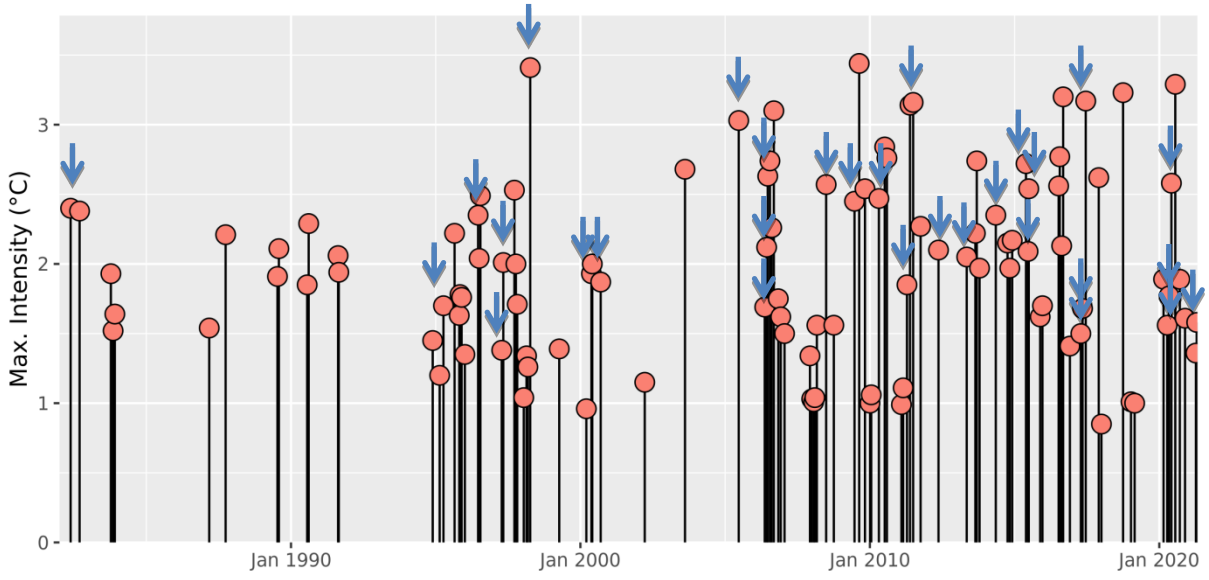

Figure 2.9: Occurrence and intensity of MHWs in the area adjacent to Ria Formosa from 1982 to the present day. Blue arrows show MHWs occurring in the April-June period. (Adapted from the Marine Heatwave Tracker app; Schlegel, 2020)

MHWs can happen at any time of the year, especially in the last decade, when their occurrence kept increasing (Figure 2.9). Several MHW events have occurred in RF area in the past years during the April-June period, and all of them were of Moderate intensity. As an example, the last one occurred from 06-04-2021 to 01-05-2021, lasted 26 days and was classified as Moderate (I), using the Hobday et al. (2018) classification, with a peak temperature at 18.16 °C. Although these moderate-intensity MHWs occurred frequently, they did not lead to massive seagrass extinction in this area. Nonetheless, there is a global trend toward increasing the frequency of Strong intensity (category II) MHWs (Hobday et al., 2018). Moreover, the temperature in Ria Formosa's shallow areas can increase dramatically (João Silva, personal communication), until locally reaching the temperature corresponding to MHWs of levels III and IV (Severe and Extreme). An event of level IV (highest level; Severe) was chosen in this experiment, to simulate the extremely high temperatures of shallow waters and observe its impacts on the seagrass' metabolism, as a simulation of what is likely to happen in the future according to the MHWs prediction scenarios (Field et al., 2012).

Following the heatwave characterization and classification proposed by Hobday et al. (2018) (Figure 2.10), a MHW of Severe intensity (category IV) is characterized by a peak temperature reaching at least 4x the 90th percentile difference from the mean regional climatology value. We applied this principle to the extrapolated Ria Formosa's temperature dataset (Figure 2.11).

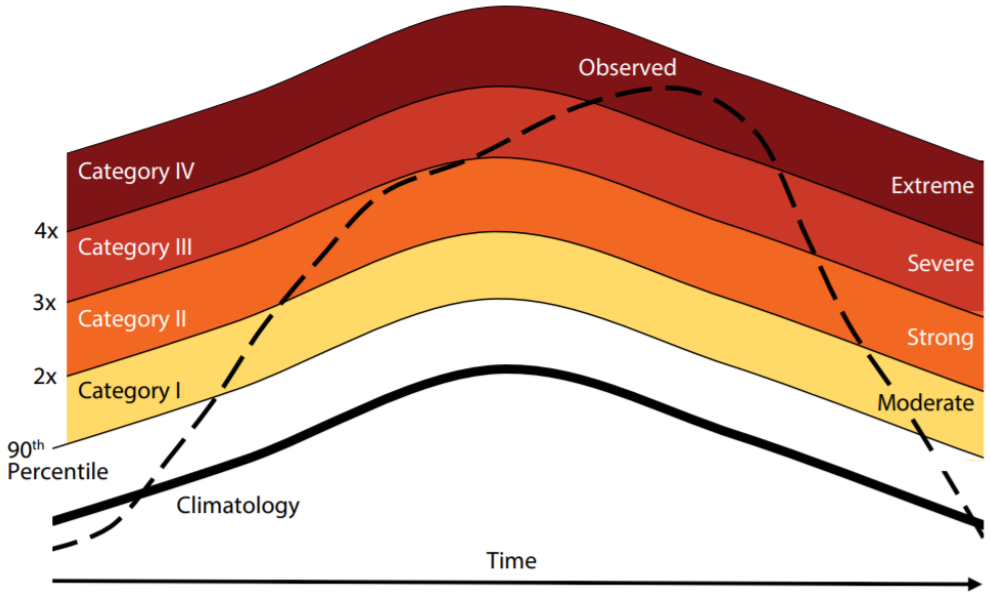

Figure 2.10: Classification scheme for MHWs, showing the observed temperature time series (dashed line), the long-term regional climatology (bold line), and the 90th percentile climatology (thin line). Multiples of the 90th percentile difference (2x: two times, 3x: three times, and 4x: four times) from the mean climatology value define categories I–IV, with corresponding descriptors from Moderate to Extreme. (In Hobday et al., 2018)

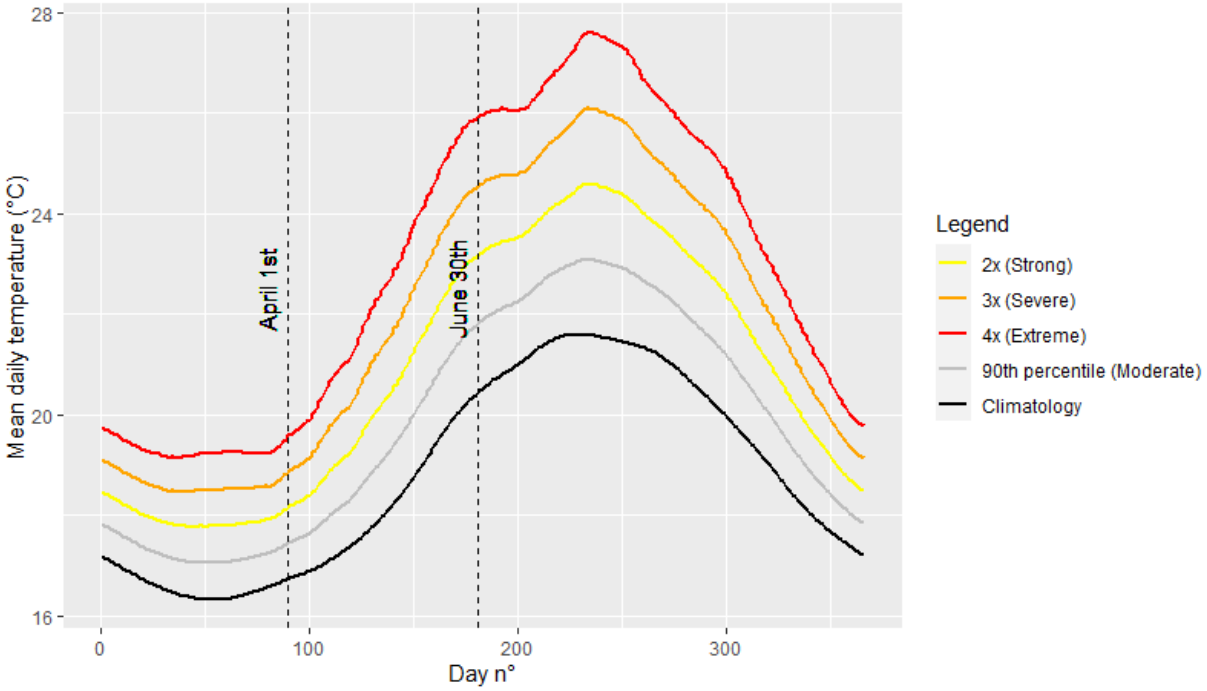

Figure 2.11: MHWs classification by Hobday et al. (2018) applied to the extrapolated Ria Fomosa's temperature data. Ria Formosa's climatology (black), 90th percentile (grey), multiples of the 90th difference (2x, 3x and 4x, yellow, orange and red, respectively) from the mean climatology value. Coloured lines represent the minimum temperature of the corresponding interval (e.g., the orange line is the minimum temperature for a MHW of Severe intensity (category III). A MHW of Severe intensity has its peak temperature between the orange and the red line). A MHW of Extreme intensity (category IV) is defined by a peak temperature above the red line.

Between April 1st and June 30th, a MHW of Severe intensity in Ria Formosa has its peak temperature at, at least, 25,9°C (Figure 2.11). However, as said before, temperature can increase dramatically above this value in some shallow areas of Ria Formosa, such as the smaller channels. Hence, choosing 28 °C as the peak temperature is relevant to simulate a Severe-intensity MHW in Ria Formosa's shallow water conditions.

According to the definition given by Hobday et al. (2016), MHWs last at least five days and heat spikes lasting less than five days are not considered as MHWs. A MHW is "anomalously warm" (temperature above the threshold, e.g., 90th percentile of climatology, which relies on data from the last 30 years, if possible), "discrete" (at least five days), and "prolonged" (with well-defined start and end times). Gaps of two days or less between events with subsequent five-days (or more) events are considered as ongoing events (Hobday et al., 2016). All metrics to characterize MHWs are classified in Table 2.1 (from Hobday et al., 2016).

Table 2.1: Hierarchical classification of metrics used to characterise MHWs. (In Hobday et al., 2016)

	Name	Definition		Units
Primary	Climatology	T_m: The climatological mean, calculated over a reference period, to which all values are relative	$T_m(j) = \sum_{y=y_s}^{y_e} \sum_{d=j-5}^{j+5} \frac{T(y,d)}{11(y_e-y_s+1)}$ where j is day of year, y_s and y_e are the start and end of the climatological base period respectively, and T is the daily SST on day d of year y	°C
	Threshold	$T_\%$: The seasonally varying temperature value that defines a MHW (e.g. T_{90} is the 90th percentile value based on the baseline periods)	$T_{90}(j) = P_{90}(X)$ where P_{90} is the 90th percentile and $P_{90}(X)$ where $X = \{T(y,d) \mid y_s \leqslant y \leqslant y_e, j-5 \leqslant d \leqslant j+5\}$	°C
	Start and end of MHW	t_s, t_e: dates on which a MHW begins and ends	t_s is the time, t, where $T(t) > T_{90}(j)$ and $T(t-1) < T_{90}(j)$ t_e is the time, t, where $t_e > t_s$ and $T(t) < T_{90}(j)$ and $T(t-1) > T_{90}(j)$ For MHWs, $t_e - t_s \geqslant 5$, and where gap $\leqslant$2 days (see text)	days
	Duration	D: Consecutive period of time that temperature exceeds the threshold	$D = t_e - t_s$	days
	Intensity (max/ mean/variance)	i_{max}: highest temperature anomaly value during the MHW	$i_{max} = \max(T(t) - T_m(j))$	°C
		i_{mean}: mean temperature anomaly during the MHW	$i_{mean} = \overline{T(t) - T_m(j)}$	
		i_{var}: variation in intensity of the MHW over the duration	$i_{var} = \sigma_{T(t)}$ where $t_s \leqslant t \leqslant t_e, j(t_s) \leqslant j \leqslant j(t_e)$, σ is the standard deviation, and the overbar indicates the time mean	
Secondary	Rate measures	r_{onset}: rate of temperature change from the onset of the MHW to the maximum intensity	$r_{onset} = \frac{i_{max} - (T(t_s-1) - T_m(j-1))}{t_{max} - (t_s-1)}$	°C/day
		$r_{decline}$: rate of temperature change from the maximum intensity to the end of the MHW	$r_{decline} = \frac{i_{max} - (T(t_e) - T_m(j))}{t_e - t_{max}}$ where t_{max} is the time of MHW_{imax}	
	Cumulative measure	i_{cum}: sum of daily intensity anomalies. Note that the integral omits t_e which is below the T_{90} threshold	$i_{cum} = \int_{t_s}^{t_e-1} (T(t) - T_m(j))dt$	°C days
	Spatial extent	A: Area of ocean meeting the MHW definition	A = area over which MHW detected	km^2
		L: Length of coastline for the MHW	L = length of coast where MHW detected	km
Tertiary	Preconditioning factors	Factors such as time of year relative to the onset of the MHW, or periods of above mean temperature preceding the MHW may lead to greater impacts	n/a	Various – specific to study system

Thus, the MHW simulated in our mesocosm system was designed with a seven-days duration and a peak temperature of 28 °C to simulate a spring-like MHW event of Severe intensity in Ria Formosa. Temperature was increased from 20 °C to 28 °C, by 1 °C a day during eight days ("*warming ramp*"), maintained at 28 °C for seven days ("*heatwave*"), and then decreased back to 20 °C by 1 °C a day ("*cooling ramp*"). Then, plants were allowed to recover from the heatwave during seven days at 20°C ("*recovery*").

2.3. Sampling design

Mature leaf samples (the 2nd or 3rd youngest) were collected from each tank (HW, *n*=5 and C, *n*=5) at the end of the heatwave (i.e., after 7 days at 28°C; "*heatwave"*) and at the end of the recovery period ("*heatwave recovery*"; Figure 2.12). Samples (*n*=20) were processed for analysis of Photosynthesis-Irradiance (P-I) curves, chlorophyll fluorescence imaging (CFI), biochemical oxidative stress indicators and measurement of the area *vs* dry weight (DW) ratio. A fraction of each sample was used to measure the fresh weight (FW) *vs* DW ratio to express the results per dry weight.

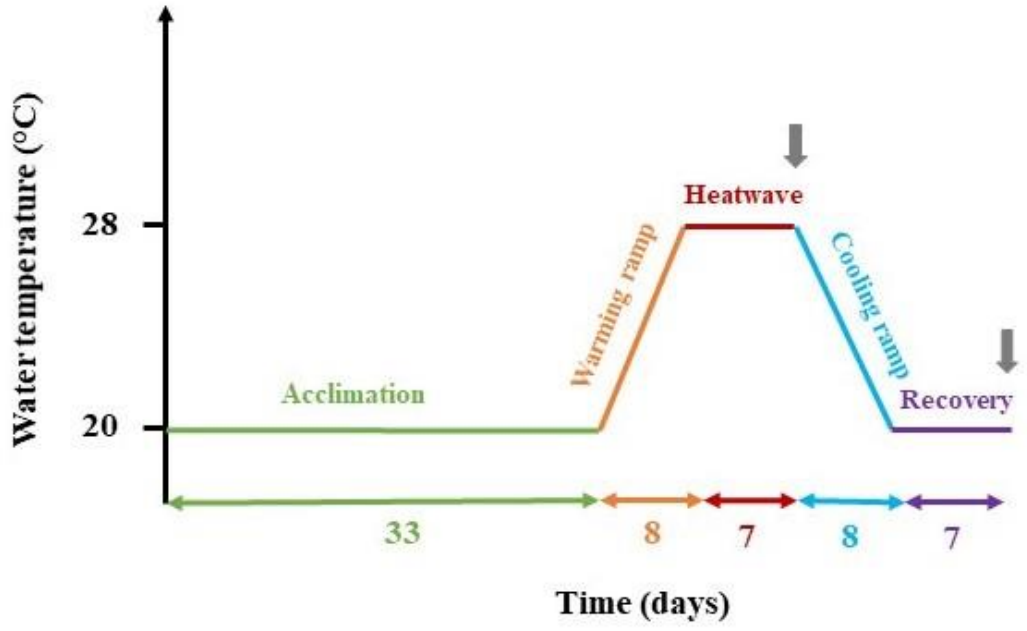

Figure 2.12: Scheme of the experimental schedule; water temperature as a function of time. *Acclimation*, *warming ramp*, *heatwave*, *cooling ramp*, *recovery*, and respective duration on the x-axis (in days). Grey arrows indicate the two sampling times.

2.4. Photosynthetic activity

2.4.1. Photosynthesis-Irradiance (P-I) response curves

P-I curves (n = 4) were performed accordingly to Silva et al. (2013), after the heatwave peak (HW, C) and after heatwave recovery (HW/R, C/R). The setup, installed right next to the mesocosm facility, was composed of five independent chambers, each with a round plastic PVC chamber filled with water from the aquaria and sealed with a petri dish containing an optical O_2 sensor (Presens Spot PS; Figure 2.13).

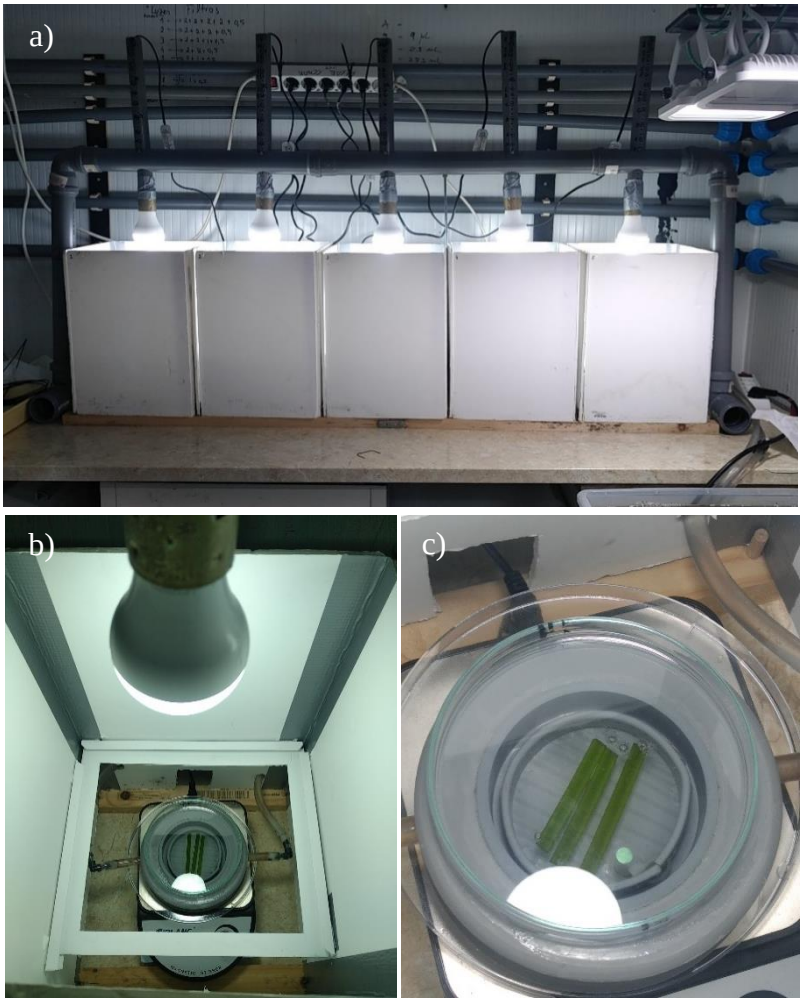

Figure 2.13: Pictures of the setup used to make the P-I curves. a) five independent chambers with respective light source; b) top-view of one chamber, showing the PVC incubation chamber, magnetic stirring, and squared frame to install the density filters; c) zoom of the top of one incubation chamber, with leaf samples placed horizontally and apparent O_2 sensor (green dot).

Water temperature inside the chambers was kept at 28 °C (HW) and 20 °C (C, HW/R, C/R) by a closed-circuit thermostatic water-bath temperature controller (Julabo HC, Julabo Labortechnik, Seelbach, Germany). A magnetic stirrer ensured water homogenization inside the chambers. Light energy was provided by five LED lamps, whose irradiance was previously measured with a Li-Cor LI-190 cosine quantum sensor (LI-COR, Lincoln, NE, USA). Combinations of neutral density filters were used to obtain the different light intensities needed. Leaf samples were cleaned from epiphytes, the middle part was cut into 3 segments (≈ 5 cm long) and then placed side by side inside the chambers to ensure their even exposure to light. Leaf segments were incubated inside the chambers under increasing photosynthetically available radiation (PAR), with ten light levels ranging from 0 to 1372 μmol photons m^{-2} s^{-1} (HW) and from 0 to 1372 μmol photons m^{-2} s^{-1} (C, HW/R, C/R). Light intensities used for measurements were chosen beforehand to draw an accurate P-I curve shape. The incubation time was adjusted from 30 to 5 min to get consistent O_2 concentration data required to draw the P-I curves. O_2 concentration (μmol L^{-1}) was measured in each chamber, firstly after 20-30 min incubation in the dark (dark respiration, DR) and then under each light intensity (net photosynthesis, NP) with a Microx 4 PreSens Optode (Regensburg, Germany). Gross photosynthesis (GP) was then calculated from NP and DR. Photosynthesis rates (DR, NP and GP; μmol O_2 gDW^{-1} h^{-1}) were calculated as follows:

$$DR, NP = \frac{\frac{[O_2]_f - [O_2]_i}{T} \times V}{DW}$$

$$GP = NP + DR$$

Where:

$[O_2]_f$ = Final O_2 concentration (μmol L^{-1})

$[O_2]_i$ = Initial O_2 concentration (μmol L^{-1})

T = Incubation time (h)

V = Volume of the chamber (L)

DW = Dry weight of the leaf tissue (g)

During the measurements, O_2 saturation levels were checked from time to time, and incubation time was adjusted to avoid O_2 supersaturation in the chamber, which can inhibit photosynthesis and involve pH changes (Beer et al., 2001; Silva & Santos, 2004).

As mathematical models do not allow to work with negative values, GP data were used to make the P-I curves. GP was fitted using the following P-I model equations: Jassby and Platt (1976), Smith (1936) and Talling (1957) and Bannister (1979) (Henley, 1993). Curve fitting was perfomed for the following equations (SigmaPlot for Windows version 14.0, 2017 Systat Software, Inc.):

Jassby and Platt (1976)	Smith (1936) and Talling (1957)	Bannister (1979)
$P = P_m \tanh\left(\frac{\alpha I}{P_m}\right)$	$P = P_m[\alpha I/\left({P_m}^2 + (\alpha I)^2\right)^{\frac{1}{2}}$	$P = P_m[\alpha I/(({P_m}^c + \alpha I)^c)^{\frac{1}{c}})]$

Where:

P: Photosynthetic rate (µmol O_2 gDW^{-1} s^{-1})

P_m: Maximum photosynthetic rate (µmol O_2 gDW^{-1} s^{-1})

I: Irradiance (µmol photons gDW^{-1} s^{-1})

α: Ascending slope at limiting irradiances, or photosynthetic quantum efficiency (µmol O_2 µmol $photons^{-1}$)

c: Curvature parameter for the Bannister equation

The model with the best fit (i.e., with the highest R^2) was used to calculate P_m, α and the half-saturation irradiance I_k (µmol photons m^{-2} s^{-1}), according to the following equation:

$$I_k = \frac{P_m}{\alpha}$$

2.4.2. Chlorophyll fluorescence imaging (CFI)

The CFI was done right after leaves sampling, to avoid the leaves drying out, using an IMAG-K2 Imaging-PAM Fluorometer (M-Series Chlorophyll Fluorescence System, WALZ, Germany). A 0.8 s saturating light pulse (ca. 5000 µmol photons m^{-2} s^{-1}) was applied to each sample immediately before taking the image.

The effective quantum yield of electron transport through photosystem II (Φ_{PSII}) is widely used to assess the level of plant stress in seagrasses (Beer et al., 2001), as is it highly sensitive to stress. Φ_{PSII} in ambient light conditions was computed from each image by "point measurements", according to the following equation (Genty et al., 1989):

$$\Phi_{PSII} = (F'_m - F_s)/F'_m = \Delta F/F'_m$$

Where:

F'_m: Maximum fluorescence of the light-adapted leaf tissue

F_s: Steady-state fluorescence of the light-adapted leaf tissue

For each leaf sampled, three images were taken, one per tissue age (young, mature and old). For each tissue age, three replicates of areas of interest (AOI) were selected on the leaf's image to calculate mean Φ_{PSII}.

2.5. Oxidative stress indicators

Antioxidant biochemical indicators (total phenolic content, TPC, oxygen radical absorbance capacity, ORAC, and Trolox® equivalent antioxidant capacity, TEAC) and oxidative damage (malondialdehyde, MDA) were investigated. Following sampling, leaf samples were carefully cut in the middle, to avoid the influence of tissue age, cleaned from epiphytes, rinsed with distilled water, blotted dry, frozen in liquid nitrogen and stored at – 80 °C until analysis.

Phenolic extracts were prepared according to Costa et al. (2021). 0.15 g of frozen leaf samples were powdered in N_2(l) and suspended in 2.5 mL HCL 0.1N. The suspensions were left overnight, in the dark and under constant shaking at 4°C; the suspensions were then centrifuged (4700 xg, 30 min, 4 °C), and the supernatant was collected. The pellet was resuspended in HCl 0.1N, centrifuged, and the supernatant collected and added to the first one. The final solution was brought to a final volume of 5 ml with HCL 0.1N. These extract solutions were used to quantify the total phenols content, ORAC and TEAC. A second extraction was done for MDA quantification.

2.5.1. Antioxidant activity

2.5.1.1. Total phenolic content (TPC)

TPC is a widespread method to measure the amount of phenols in all types of food and plant extracts (Shahidi & Zhong, 2015). According to Booker & Miller (1998), TPC was quantified using the Folin-Ciocalteu method (Folin & Ciocalteu, 1927). This assay relies on the reduction of the Folin–Ciocalteu reagent by phenolic compounds in alkaline conditions. A calibration curve was made before samples readings, using several dilutions of a chlorogenic acid stock solution (200 µg mL^{-1}). 42 µL of phenolic extract/calibration solution was added to 0.4 mL Folin-Ciocalteu reagent 0.25 N. 3 min later, 0.4 mL of NA_2CO_3 7.5% was added. Blank solutions were made with HCl 0.1N instead of extract for the samples, and Mili-Q water for the calibration curve. Cuvettes were placed in the dark for 60 min and then read in the spectrophotometer at 724 nm (Booker & Miller, 1998). Phenolic compounds' concentration was calculated as chlorogenic acid equivalents in µg of chlorogenic acid per gDW.

2.5.1.2. Trolox® Equivalent Antioxidant Capacity (TEAC)

The TEAC assay is widely used to measure the total antioxidant activity of pure substances, body fluids and plant materials (Shahidi & Zhong, 2015). It quantifies the protection capacity against peroxyl radicals (ROO•) through total antioxidant capacity based on a single electron transfer. This assay is based on the use of a blue-green radical cation chromophore ($ABTS^{\bullet+}$; 2,2′-azinobis (3-ethylbenzothiazoline-6-sulphonic acid)) with maximum absorption at 734 nm which, when added to antioxidant compounds, is inhibited and leads to the decolourization of the solution (as a function of antioxidant activity, concentration and reaction time). Decolourization is measured as a percentage of inhibition of the $ABTS^{\bullet+}$ radical cation (Re et al., 1999; Huang et al., 2002).

An oxidised $ABTS^{\bullet+}$ solution was prepared by adding potassium persulfate to a 7mM ABTS solution for a final concentration of 2.45 mM potassium persulfate. Right before the assay, the $ABTS^{\bullet+}$ solution was diluted in ethanol to obtain an absorbance reading of 0.8 ± 0.02 at 734 nm. A 2.5 mM Trolox stock solution was prepared in ethanol and then diluted several times to obtain standard solutions of different concentrations. 990 µl of the

$ABTS^{\bullet+}$ solution was read at 734 mm (A_0). Then, 10 µl of each Trolox® standard solution/phenolic extract was added, mixed, let to rest 6 min and read at 734 nm (A_1).
% Absorbance inhibition was calculated using the formula:

$$\%\ Absorbance\ inhibition = \frac{A_0 - A_1}{A_0} \times\ 100$$

Where:
A_0: Absorbance of the $ABTS^{\bullet+}$ solution
A_1: Absorbance of the Trolox® standard/phenolic extract

% Absorbance inhibition for each Trolox® standard was used to build a calibration curve. Sample TEAC concentration was then calculated as µM of Trolox® equivalents (with linear regression equation: $y = ax + b$) and expressed as µM Trolox® equivalents per gram of DW, according to the following equation:

$$TEAC\ concentration\ (\mu M\ Trolox^{®}eq\ ) = \frac{\%\ Absorbance\ inhibition - b}{a}$$

2.5.1.3. Oxygen Radical Absorbance Capacity (ORAC)

Peroxyl radicals (ROO•) are considered the major free radicals responsible for lipid oxidation (Shahidi & Zhong, 2015). The ORAC assay quantifies the protection capacity against peroxyl radicals through hydrogen atom transfer (HAT). It measures the antioxidant inhibition of peroxyl radical-induced oxidations and accounts for the measurement of the antioxidant capacity of phenolic compounds and tocopherols. The method relies on the reaction of peroxyl radicals with a fluorescent probe (fluorescein, Sigma) and the consequent loss of fluorescence is recorded with a fluorometer. The ORAC analysis was done following the protocols of Gillespie et al. (2007) and Huang et al. (2002), using ABAP (2,2-azobis(2-amidinopropane) hydrochloride, Sigma) instead of AAPH (2,2′-azobis(2-amidinopropane) dihydrochloride) as a lipophilic peroxyl radical generator.

A 75 mM potassium phosphate buffer solution, pH 7.4, was prepared with K_2PO_4 and KH_2PO_4 in Mili-Q water. The phosphate buffer was then filtered with a 0.22 µm nylon.

An 8.2 x 10^{-5} mM fluorescein stock solution was prepared in the phosphate buffer. A 0.02 M Trolox® stock solution was made in phosphate buffer, and then six standard solutions were prepared (concentration range: 0 to 100 µM). A 153 mM ABAP solution was prepared in phosphate buffer right before use. As the reaction of peroxyl radicals is sensitive to temperature (Prior et al., 2005), the microplate reader (Synergy TM 4 multi-detection microplate reader with a 485 nm excitation filter, 20nm bandpass, and a 528 nm excitation filter, 20 nm bandpass) was pre-heated at 37°C half an hour before use. 200 µL of buffer solution was put in the frame wells of a 96-well microplate to maintain the temperature stability. In the other wells, 25 µL of each sample/blank/standard solution was added in triplicate, and then 150 µL of fluorescein stock was added and put to agitate in the microplate reader. Finally, 25 µL of freshly prepared ABAP solution was added. The net integrated area below the decay curve was then calculated, accounting for the indicator of the peroxyl radical scavenging capacity of the antioxidants (Figure 2.14). The results were expressed as µM Trolox® equivalents per gram of DW.

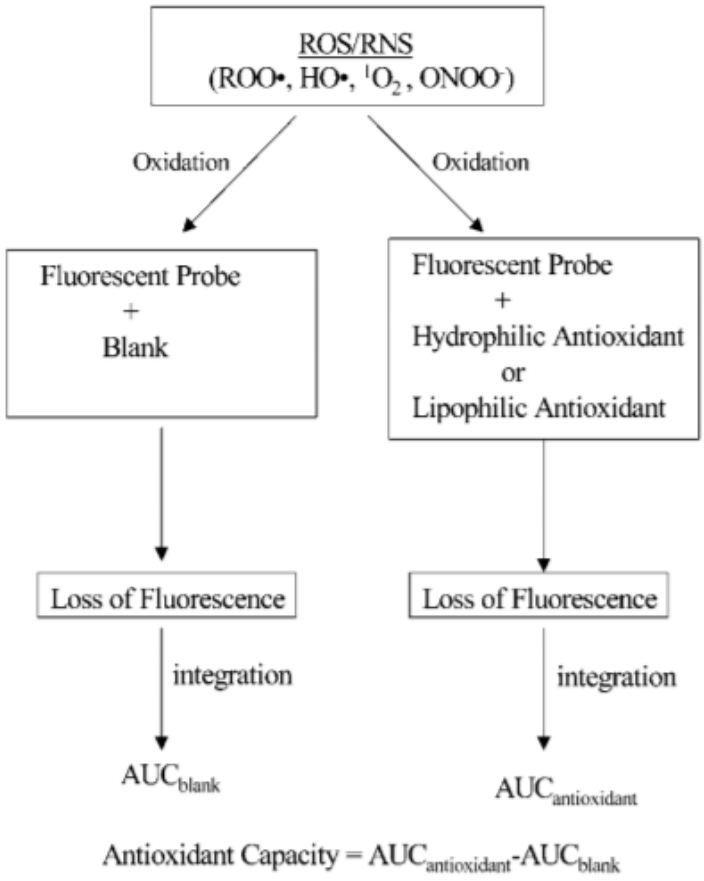

Figure 2.14: Schematic illustration of the principle of the ORAC assay. (In Huang et al., 2002)

2.5.2. Oxidative damage: MDA quantification

MDA is a final secondary product of polyunsaturated fatty acids autooxidation (responsible for cell damage) and enzymatic degradation. Hence, it is considered a valuable indicator of lipid peroxidation under oxidative stress (Hodges et al., 1999). This assay relies on the reaction of MDA with two molecules of thiobarbituric acid (TBA), yielding a red chromogen with an absorption peak at 532 nm. Due to the presence of sugars, Du & Bramlage (1992) modified the traditional MDA assay of Heath & Packer (1968) by subtracting the absorbance at 440 nm from the one at 532 nm. Another reading at 600 nm is traditionally made to correct the readings for non-specific absorbance due to turbidity. Some other compounds, which concentration vary from plant to plant and with stress level, interfere with reading at 532 nm leading to MDA overestimation (Taulavuori et al., 2001), which can reach up to 96.5% in some plants (Hodges et al., 1999). To overcome this issue, absorption at 532 nm is measured both for a solution containing plant extract with TBA and another without TBA, according to Hodges et al. (1999).

300 mg of frozen leaf tissue was ground in liquid nitrogen, suspended in 5 mL ethanol 80%. After homogenisation, the extracts were centrifuged at 3000 xg for 10 min. The supernatant was added to a 20% trichloroacetic acid with 065% TBA and 0.015% butylated hydroxytoluene. Two blank solutions were made either without TBA or with ethanol 80% instead of sample extract. After mixing well, all samples and blanks were incubated at 90 °C for 25 minutes, then cooled down in ice for 15 minutes, and centrifuged at 3000 xg for 10 minutes. The supernatant absorbances (Abs) were read at 440, 532 and 600 nm with the spectrophotometer (Novaspec Plus, Healthcare Bio-Sciences AB, Uppsala, Sweden), and MDA equivalents per gram of DW were calculated as follows (Hodges et al., 1999):

1) $(Abs_{532+TBA} - Abs_{600+TBA}) - (Abs_{532-TBA} - Abs_{600-TBA}) = A$

2) $(Abs_{440+TBA} - Abs_{600+TBA}) \times 0.0571 = B$

3) $\text{Eq MDA (nmol mL}^{-1}) = \frac{A - B}{157\,000} \times 106$

4) $\text{MDA (nmol gDW}^{-1}) = \text{Eq MDA} \times \frac{V_{final}}{V_{aliquote}} \times V_{extraction} \times \frac{1}{DW}$

Where:

DW : Dry weight of the leaf tissue (g)

V: Volume of the different solutions (mL)

2.6. Leaf area *vs* dry weight ratio

To investigate the impact of the MHW on the leaves' biomass, the area *vs* DW ratio of the leaves was calculated. Leaf segments used for the P-I curves were readily photographed for later measurement of their surface area (m^2) with the ImageJ software (Rasband, 2018). Then, the DW (g) of each sample was measured after drying in the oven at 60 °C for at least 48 h.

2.7. Statistical analysis

All statistical analyses were performed using R Studio software (R Core Team, 2014). Beforehand, data were tested for normality (Shapiro-Wilk's test) and homogeneity of variances (Levene's test). Differences between treatments (HW *vs* C) at both sampling times ("*heatwave*" and "*heatwave recovery*") were tested using one-way analysis of variance (ANOVA). Whenever the hypothesis of homogeneity of variance was rejected, a Welch ANOVA test was performed, followed by a Games-Howell posthoc test. To investigate the coupled effects of tissue age and treatment on Φ_{PSII}, a two-ways ANOVA was performed. In case of the absence of significant interaction between the two factors, two one-way ANOVAs were performed to search for any significant difference in Φ_{PSII} between leaf parts and between treatments, independently. If significance was detected, a Tukey-HSD test was performed for pairwise comparison of the factors "leaf part" and "treatment". For all tests, a significance level of α=0.05 was used.

3. Results

3.1. Shoots survival

For unknown reasons, most *Z. marina* shoots did not survive the transplant. Almost all leaves died or suffered from necrosis after the acclimation period and there was not enough biomass left to run the analyses (Figure 3.1). Nevertheless, *C. nodosa* survived the transplant, grew and thrived until the end of the experiment. Henceforward, only the results for *C. nodosa* will be presented and discussed.

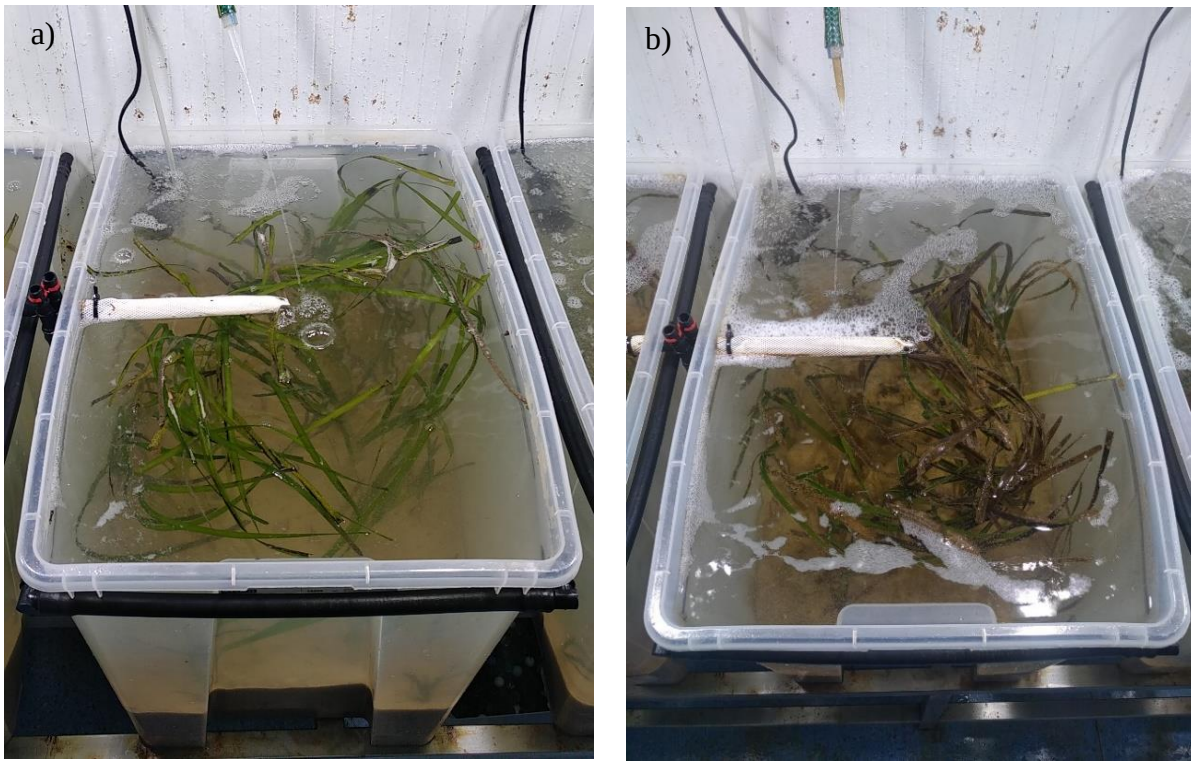

Figure 3.1: Pictures from the top of one aquarium with a mixed culture of *C. nodosa* and *Z. marina*, taken after shoots transplant (a) and after 23 acclimation days (b). After several days of acclimation in a mesocosm, shoot darkening is expected due to leaf ageing and epiphyte colonisation; however, a closer look at *Z. marina* shoots revealed just a few new leaves and several necrotic mature and old leaves.

3.2. Photosynthetic activity

3.2.1. Photosynthesis-irradiance (P-I) curves

Among the three mathematical models tested, Jassby and Platt (1976) was the most suitable for all experimental treatments (higher mean R^2=0.792; Table 3.1).

Table 3.1: P-I best fit (R^2) study for Jassby & Platt (1976), Smith (1936) & Talling (1957) and Bannister (1979) P-I model equations. n/a indicates that the data could not be fitted with this model, thus Bannister's equation could not be selected to fit the all the data. Bold indicates the best fit model to the data.

Treatment	Mathematical model		
	Jassby & Platt (1976)	Smith (1936) and Talling (1957)	Bannister (1979)
Heatwave			
HW	0,809	0,812	0,813
C	0,856	0,859	0,859
Heatwave recovery			
HW	0,661	0,691	n/a
C	0,841	0,441	0,844
Mean R^2	**0,792**	0,701	0,839

C. nodosa leaves' photosynthetic activity responded to light stimulation by a typical hyperbolic-shaped response with increasing light intensity (Figure 3.2). Under limiting irradiances, GP rates increased linearly with light until light intensity reached the half-saturation light intensity (I_k). The maximum photosynthetic rate (P_m) was reached at saturating light intensities.

Photosynthetic quantum efficiency (α, the ascending slope of the light-limited part of the P-I curve), P_m and I_k, calculated using Jassby and Platt's (1976) P-I model, are presented in Table 3.2.

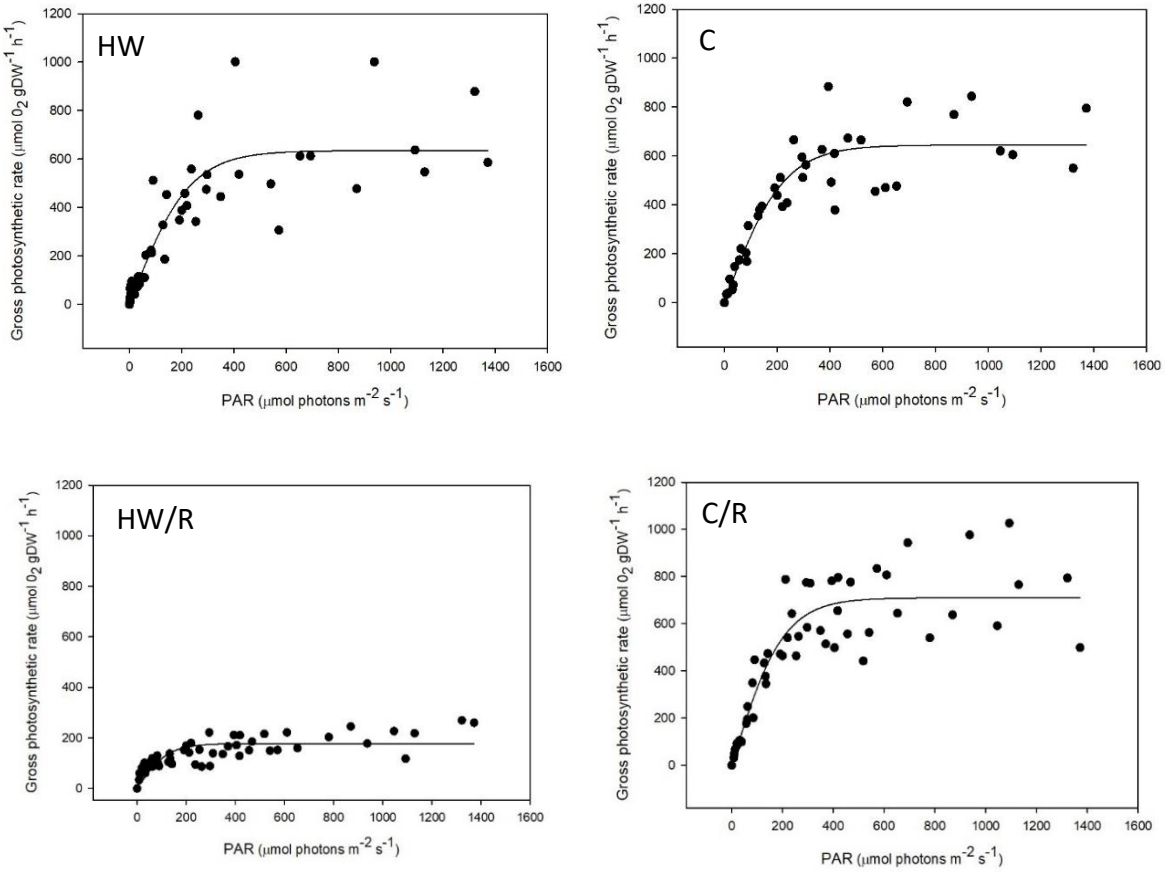

Figure 3.2: P-I curves of *C. nodosa*'s leaves sampled during the heatwave peak (heatwave, HW, and control, C) and after a 7-days recovery (HW/R and C/R), fitted with the Jassby & Platt (1976) model equation.

Table 3.2: *C. nodosa's* photosynthetic parameters obtained after fitting the data with the Jassby & Platt (1976) P-I model. Mean photosynthetic quantum efficiency (α; µmolO_2 µmol photons^{-1}), maximal photosynthetic rate (P_m; µmol O_2 gDW^{-1} h^{-1}), and half-saturation irradiance (I_k; µmol photons m^{-2} s^{-1}) are expressed as values ± SE, for each treatment, with corresponding R^2 and number of observations (*n*). The significance level is the degree of significant difference between treatments HW and C (n.s.: non-significant; *: significant, p<0.05; ***: highly significant, p<0.001), both during the heatwave and after heatwave recovery.

	Parameters				
Treatment	**α ± SE**	**P_m ± SE**	**I_k ± SE**	R^2	*n*
Heatwave					
HW	2,805 ± 0,352	635,02 ± 37,05	226,4 ± 31, 3	0,809	55
C	2,921 ± 0,305	644,9 ± 27,5	220,8 ± 24,9	0,856	44
Significance level	n.s.	n.s.	n.s.		
Heatwave recovery					
HW	1,429 ± 0,229	177,4 ± 8,1	124,2 ± 20,7	0,661	54
C	3,539 ± 0,372	709,8 ± 27,6	200,6 ± 22,5	0,841	55
Significance level	***	***	*		

α, P_m and I_k were significantly lower in leaves from plants recovering from the heatwave than control ($p<0.001$, $p<0.001$ and $p=0.008$, respectively). While α was *ca*. 2-fold times lower than control, P_m was *ca.* 4-fold times lower and therefore, I_k decreased significantly. Conversely, α, P_m and I_k were not significantly different between treatments HW and C in leaves sampled during the heatwave.

3.2.2. Chlorophyll fluorescence imaging (CFI)

During the heatwave, Φ_{PSII} was significantly higher in HW leaves than control ($p=0.008$), and old leaf tissues displayed a lower Φ_{PSI} than mature ones ($p=0.035$; Figure 3.3; Figure 3.4) in both HW and C leaves. No significant differences were found between HW and C leaves nor between tissue ages after the heatwave recovery.

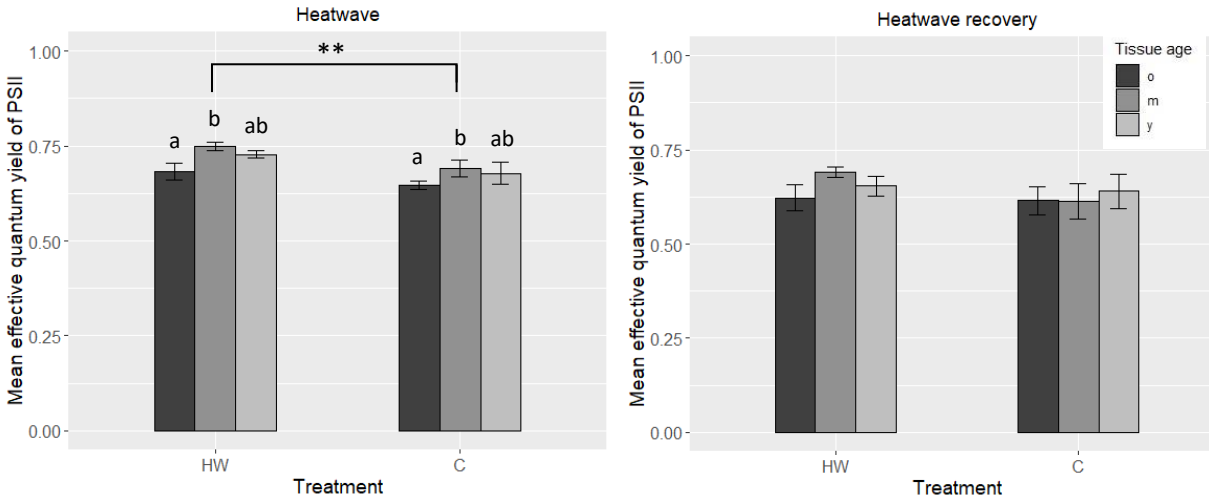

Figure 3.3: Φ_{PSII} of heatwave (HW) and control (C) *C. nodosa*'s leaf tissues, sampled during the heatwave and after heatwave recovery, for old (o) mature (m) and young (y) leaf tissues. Values are means ± SE ($n=5$). Different letters indicate significant differences between tissue ages ($p<0.05$), and ** indicates significant differences between treatments ($p<0.01$).

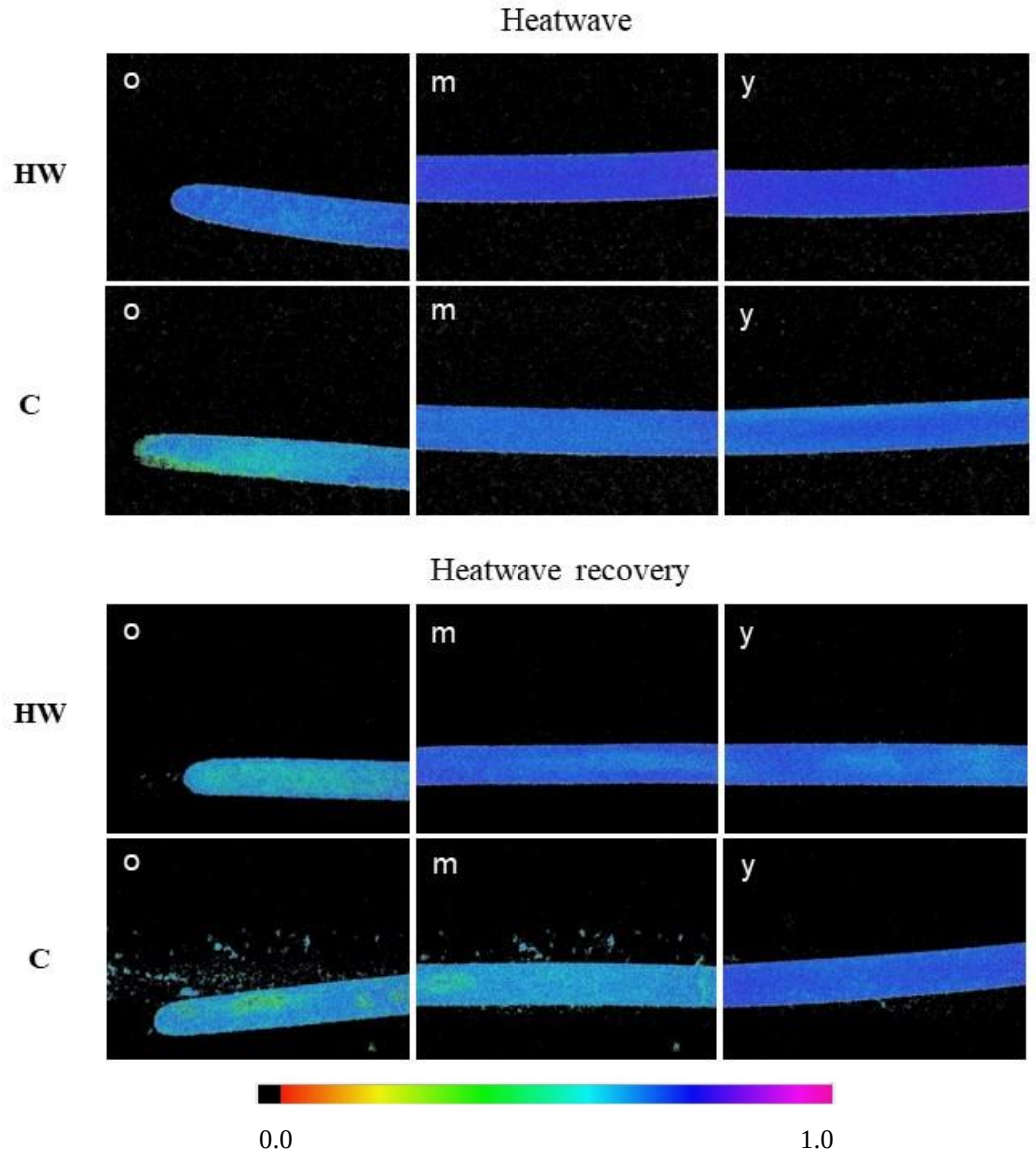

Figure 3.4: Examples of CFI pictures of *C. nodosa*'s Φ_{PSII} after a saturating light pulse, in mature leaves from shoots grown in heatwave (HW) and control (C) conditions, sampled during the heatwave and after heatwave recovery. o, m and y indicate different leaf parts (old, mature and young, respectively). Colour bar on the bottom indicates Φ_{PSII} values ranging from 0.0 (black) to 1.0. (pink). Pictures are 24x32 mm (6x magnification).

3.2. Oxidative stress indicators

Total phenols, TEAC, ORAC and MDA concentrations in *C. nodosa*'s leaf tissues are presented in Table 3.3. There was no significant variability in oxidative stress indicators concentration between treatments, neither during the heatwave simulation nor after heatwave recovery.

Table 3.3: Total phenols (mg gDW^{-1}), TEAC (µmol Trolox eq gDW^{-1}), ORAC (µmol Trolox eq gDW^{-1}) and MDA (nmol gDW^{-1}) concentrations in mature *C. nodosa*'s leaves from heatwave (HW) and control (C) tanks, during the heatwave and after recovery. Values are means ± SE and *n* is the number of replicates.

	Treatment			
	Heatwave		*Heatwave recovery*	
	HW	**C**	**HW**	**C**
Total phenols (mg gDW^{-1})	11,81 ± 1,72 *n=5*	10,93 ± 0,23 *n=4*	10,79 ± 0,92 *n=5*	10,17 ± 1,41 *n=5*
TEAC (µmol Trolox eq gDW^{-1})	9,47 ± 3,48 *n=5*	9,95 ± 3,09 *n=5*	12,22 ± 1,36 *n=5*	7,96 ± 1,83 *n=5*
ORAC (µmol Trolox eq gDW^{-1})	139,24 ± 34,32 *n=5*	206,01 ± 62,66 *n=5*	132,27 ± 51,08 *n=5*	126,98 ± 13,46 *n=5*
MDA (nmol gDW^{-1})	88,71 ± 20,81 *n=4*	83,49 ± 20,62 *n=4*	186,58 ± 2,14 *n=3*	100,85 ± 34,09 *n=5*

Although non-significant, total phenols and MDA concentration were slightly higher in HW leaves than C leaves during the heatwave, whereas TEAC and ORAC concentrations were slightly lower in HW leaves than control. On the other hand, total phenols, TEAC, ORAC, and MDA concentrations were slightly higher in HW leaves after heatwave recovery than control.

3.3. Leaf area *vs* dry weight ratio

C. nodosa's leaf area *vs* DW ratio was higher in HW than C leaf tissues, with significance after heatwave recovery (Figure 3.5). Hence, few days after the end of the MHW, *C. nodosa*'s leaves that went through a heatwave simulation had less biomass than those grown in control conditions.

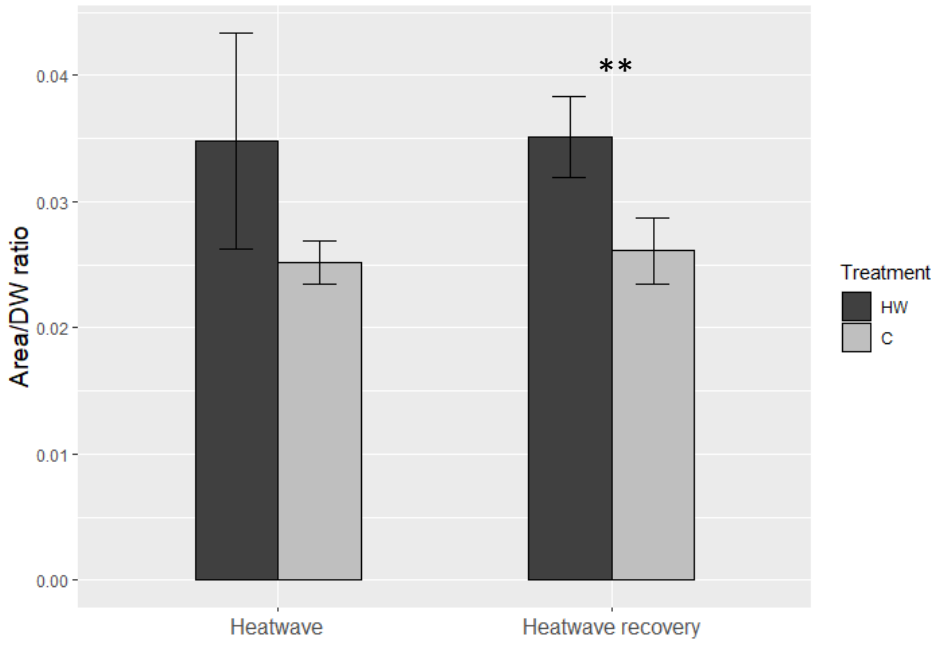

Figure 3.5: Area *vs* DW ratio of *C. nodosa*'s leaf tissues from treatment HW and C, sampled during the heatwave and after heatwave recovery. Values are means ± SD (*n=5*). ** indicates significant differences between treatments ($p<0.01$).

4. Discussion

The results of this study show that MHWs can negatively impact *C. nodosa*'s biology in the long term by lowering its photosynthetic capacity and light-saturating irradiance several days after the end of the heat stress. In this particular case (a seven-day spring heatwave peaking at 28°C), a decrease in leaf biomass was also observed. In combination with reduced photosynthetic rates and efficiency, this leaf biomass loss implies an additional reduction of the global productivity of the plants with direct consequences on growth. On the other hand, the heatwave did not imply significant oxidative damage or changes in the leaves' antioxidant system of *C. nodosa*.

Long-term adverse effects were observed on the photosynthetic performance of *C. nodosa*. While the heatwave peak only affected Φ_{PSII} significantly, the measured photosynthetic parameters only showed strong negative effects after some days of recovery at lower temperature: the maximal photosynthetic rate (P_m), the amount of O_2 released per unit of incident light (α) and the minimum-light intensity needed to reach P_m (I_k) decreased significantly after the recovery period. Conversely, no changes in these photosynthetic parameters of *C. nodosa* leaves were observed during the heatwave, showing that the effects only came out several days after the end of the heat stress. Φ_{PSII} increased significantly during the heatwave, accounting for a higher electron transport rate in the electron transport chain of photosynthesis (Maxwell & Jonhson, 2000) under heat stress. Maintaining a high electron flow can be advantageous to compensate the negative effects of heat stress and keep photosynthetic and growth rates at a constant level. Φ_{PSII} was higher in mature parts of the leaves than in old tissues, which has been shown to be a common feature related to the reduction of leaf thickness and cell layers towards the tip (Schubert et al., 2018). Nonetheless, in our work, this feature was not significant during the recovery, and this result may be related to the increased area *vs* DW ratio in heatwave recovering leaves, as discussed below. When Φ_{PSII} went back to control level several days after the heatwave, the photosynthetic performance of the plant dropped, suggesting that *C. nodosa* is only able to temporarily maintain its gross photosynthetic activity at a normal rate under thermal stress by a "compensation" response, increasing the electron transport rate through PSII during a few days. However, it is likely to be unable to sustain this metabolic compensation response in the long term, resulting in the drop of photosynthetic performance several days after the heat stress, while Φ_{PSII} comes back to control level. Costa et al. (2021) also suggested that Φ_{PSII} increases with heat stress in *C. nodosa* leaves (after a 4-days heat shock at 40 °C). This study

confirms that a short-term response to heat stress involves an increase in Φ_{PSII}, probably supporting photosynthesis during the thermal stress, be it of different length and intensity. The fact that Φ_{PSII} goes back to control level after the heatwave suggests that *C. nodosa*'s PSII has a certain ability to recover from the heat-stress damage, as revealed by Marín-Guirao et al. (2016). However, nothing suggests that *C. nodosa* would be able to recover from a more intense and long-lasting MHW, as forecasted in future climate-change scenarios.

The decrease of photosynthetic performance in leaves suggests that a higher fraction of the oxygen produced by photosynthesis is consumed during and after the heat stress, indicating the up-regulation of the oxygen-consuming process(es) such as respiration, photorespiration or Mehler reaction (reduction of the O_2 molecules in PSI when there is an excess of electrons in the chain, possibly due to the increased activity of PSII). The increment of these oxygen-consuming processes can enhance the production of reactive oxygen species (ROS) such as H_2O_2 and superoxide radicals (Mehler, 1951; Apel & Hirt, 2004). Although it has been reported that thermal stress induces the production of ROS in submerged macrophytes (Chalanika De Silva & Asaeda, 2017), the putative consequences of increased oxidative stress (membrane lipid peroxidation measured as MDA) and the ROS scavenging capacity (TEAC and ORAC) presented no significant changes during and after the heatwave, showing no general increase in the concentration of antioxidant species in *C. nodosa* leaves. Similarly, the unchanged MDA values show that the possible increase in ROS did not provoke oxidative stress, meaning that the existing antioxidant system of *C. nodosa* was probably sufficient to avoid oxidative damage.

Although non-significant, total phenols, TEAC, ORAC and MDA concentrations were slightly higher in leaves recovering from the MHW than control. While the short-term effects of the heatwave on biochemical oxidative-stress indicators were not clearly shown in this experiment, the long-term consequences appear to be more relevant. These results suggest that the oxidative stress of *C. nodosa* is more detectable after heatwave recovery than during the heatwave itself. This could be interpreted as a long-term acclimation response of *C. nodosa*'s biochemistry to the potentially low oxidative stress caused by the prolonged heat stress. Costa et al. (2021) suggested that short and intense heat stress (40 °C for 4 days) implies a significant increase in *C. nodosa*'s antioxidant response (measured with TEAC). The non-significance of our results may be justified by the characteristics of the MHW, which, in Costa et al. (2021), was more intense and suddenly imposed, whereas in the present work, the MHW was progressively imposed and less intense. The absence of oxidative

damage under a short and intense heat shock, as reported in Costa et al. (2021), is in line with our results. Indeed, MDA concentration does not seem to increase in *C. nodosa* when the plants are exposed to thermal stress, suggesting that *C. nodosa* is resistant to the stress caused by MHWs of different lengths and intensities. Nonetheless, foliar MDA is slightly higher after recovery from a prolonged heatwave (around 190 nmol gDW^{-1}; present study) than right after a short and intense heat shock (around 100 nmol gDW^{-1}; Costa et al., 2021). These results suggest that oxidative damage, if there is, is more likely to be critical in plants recovering from heatwave-type stress (more extended heat stress, long-term effect) than right after a short heat shock. *C. nodosa* seems to have a relatively high oxidative-stress tolerance, notably comparing to *Z. marina* in the same thermal environment (Tutar et al., 2017). In Ria Formosa, *C. nodosa* seems to have a sufficient antioxidant capacity to cope with stress induced by a spring MHW. A longer and/or more severe MHW (e.g., of Extreme intensity; Hobday et al., 2018) for this time of the year may increase more significantly the oxidative stress and cell damage in *C. nodosa* leaves, possibly with irreversible damages.

This study showed that the simulated MHW impacted the morphology of *C. nodosa*'s leaves. The area *vs* DW ratio suggested that the heatwave induced a decrease in leaf biomass, especially several days after the end of the heatwave. *C. nodosa* might have responded to the thermal stress by possibly reducing its leave's thickness, which could be explained by a lower growth rate, resulting in decreased photosynthetic tissue and, therefore, a lower photosynthetic performance. Another possibility is the increase of the size of the aerenchyma (air channels inside the leaves). These lacunae act as either sources or sinks for O_2 (Beer et al., 2001; Brodersen et al., 2018), and an increase in their volume could be related to a higher O_2 transfer inside the plant, (from leaves to roots and rhizomes) together with enhanced electron transport (as seen before) or stand for a more intense gas exchange for respiration/photorespiration processes. Cross-section analysis of *C. nodosa*'s leaves, such as in Schubert et al. (2018), would be helpful to further investigate the effect of MHWs on the leave's anatomy and, more precisely, observe changes in the size of the aerenchyma.

The present study investigated the effects of a particular spring-like MHW in Ria Formosa on *C. nodosa* shoots. Results must not be extrapolated for all-year-round conditions or for shoots coming from different thermal environments (temperate or tropical/subtropical). In fact, the optimum temperature for seagrass growth and photosynthesis does not only varies between species but also between individuals of the same species coming from different origins (Lee et al., 2007), and metabolic responses of the plants to MHWs can greatly vary with their historic

thermal environment (Franssen et al., 2014; Beca-Carretero et al., 2018, 2020; Marín-Guirao et al., 2018). Seagrasses may have different responses to MHW, when these events occur at different times of the year (summer or winter), as the plant's metabolism follows a seasonal pattern (Pérez & Romero, 1992). Also, in the case of reoccurrence of MHW events in a relatively short time, *C. nodosa* and other seagrass species are likely to be more susceptible and more critically affected by heat stress. In fact, Saha et al. (2020) showed that cumulative heatwave events had a negative impact on the growth and leaf production rate (*i.e.*, biomass) of *Z. marina,* whereas an isolated MHW event did not induce any significant change in the plant's biology.

Egea et al. (2019) showed that a 2°C temperature increase during a short period (precisely, from 24 to 26°C for 24 h) had a positive effect on the productivity of *C. nodosa*, enhancing the whole community's dissolved organic carbon fluxes. They suggested that the autotrophy of a *C. nodosa* meadow community was triggered by a thermo-enhanced metabolic activity, intensifying its role as a carbon sink, which might not be pointed out when studying isolated plants. Furthermore, the productivity of *C. nodosa* beds might be boosted by a temperature increase within its optimum but negatively affected by a higher and/or longer-lasting temperature rise. Costa et al. (2021) suggested that P_m was lower in Ria Formosa's plants that had suffered from intense thermal stress (4 days at 40°C) than in plants kept at 20 °C. While both a 4-days heat shock at 40°C and our 7-days heatwave at 28°C had negative consequences on the photosynthetic activity of *C. nodosa* in Ria Formosa, the responses seem to appear at different time scales (short-term and long-term, respectively). We suggest that a prolonged, but less intense temperature rise (namely the heatwave), may have long-term consequences on the plant's photosynthetic activity, whereas a short, although more intense heat stress, involves an immediate decrease of P_m, and with it, the immediate drop of photosynthetic efficiency.

Besides photosynthetic activity and oxidative stress, MHWs can impact other parameters of the seagrasses' biology, with differences between species and thermal environments (Marín-Guirao et al., 2016). As an example, they can affect their fatty acids composition, negatively impacting their nutritional value for higher trophic levels (Beca-Carretero et al., 2018). Bergmann et al. (2010) demonstrated molecular stress by regulation of heat stress proteins (HSP) during a simulated heatwave at 26°C (simulating the 2003-European heatwave) upon *Z. marina* populations coming from different thermal regimes. As it has been demonstrated for short heat shocks on *Z. marina* plants, it is likely that MHWs also have an important

impact on a wide range of processes, such as the flowering and reproductive activity of plants, carbon storage and allocation, shifts in gene expression and metabolomic responses, variations in DNA methylation, protein folding and cell wall modification (Gu et al., 2012; Franssen et al., 2014; Tutar et al., 2017; Marín-Guirao et al., 2018; Jueterbock et al., 2020; Qin et al., 2020). However, as seagrass species show different physiological responses to MHWs, more research is needed to specifically understand their consequences on *C. nodosa*'s biology.

Overall, studies show that *C. nodosa* seems to present a higher tolerance to anomalous temperature events than other seagrass species in the same thermal environment (Olsen et al., 2012; Tutar et al., 2017; Beca-Carretero et al., 2018; Savva et al., 2018). Although *C. nodosa*'s optimal temperatures are higher than other seagrass species, a spring-like heatwave such as the 28°C one used in the present work have the potential to negatively impact the *C. nodosa* population in Ria Formosa if occurring during a period when seasonal temperatures are lower (e.g., in autumn or early spring). Investigate MHWs' effects at different times of the year is needed here, to test this hypothesis. Studies on *Z. marina* showed that growth, biomass, productivity and photosynthetic rate were reduced too under heatwave simulations and temperatures between 25-30 °C (Nejrup & Pedersen, 2008; Bergmann et al. 2010; Moreno-Marín et al. 2018; Kim et al., 2020). Hence, the distribution of both species in Ria Formosa is likely to be altered by more frequent and intense MHW events under climate change scenarios.

It is important to remind that mesocosm experiments measure the productivity of isolated *C. nodosa* plants, regardless of the whole community's production and interactions, and possible artefacts relative to the experimental setup. The effects of a MHW on isolated *C. nodosa* shoots might not be the same as on *C. nodosa* meadow's community. In this sense, *in situ* experiments are more suitable for approximating what happens in the natural environment and widening the results at a larger scale (e.g., at the whole Ria Formosa scale instead of a few plants). However, *in situ* experiments are limited to short incubation times (c.a. 24 h), as the absence of water mixing causes dissolved oxygen oversaturation and pH shifts (Egea et al., 2019). Additionally, temperature management *in situ* is more challenging, and environmental parameters vary more than in a fully controlled environment. No experimental design is perfect, and they hardly provide an accurate simulation of what occurs in the natural environment (shifts in hydrodynamic, turbidity, nutrients income, shading, eutrophication…). In nature, several biotic and abiotic parameters interact and can have coupled effects

(Moreno-Marín et al. 2018: Kim et al., 2020). Hence, analysing the effects of one parameter (here, the temperature) does not necessarily allow forecasting one species' response, and conclusions must be made with caution. Although temperature is the most important factor affecting its production, *C. nodosa* expresses a large variety of responses to different combinations of factors that can be antagonistic or synergistic (Egea et al., 2018). Therefore, multifactorial in-situ experiments are more suitable to predict the future of seagrasses. Finally, comparing the results with previous studies is difficult because of the lack of homogenization in methodologies (O_2 electrodes or Winkler titration for measuring O_2 exchange, measurement of Φ_{PSII} or ETR…), units (e.g., GP or NP, normalization per m^2 or gDW for the photosynthetic rate), and experimental design. Moreover, both the fluorescence and the O_2 gas exchange method have their own drawbacks and relevant sources of errors (reviewed in Beer et al., 2001). Hence, comparisons must be taken carefully.

5. Conclusions

In the present study, *C. nodosa* shoots from Ria Formosa showed a certain tolerance to a spring-like MHW event. The increased frequency and intensity of MHWs may not have dramatic effects on the biology and survival of *C. nodosa* in the short term, as this species can keep up with its photosynthetic performance and is tolerant to oxidative stress. However, there is evidence that heatwaves can affect *C. nodosa*'s biology in the long term by negatively impacting its photosynthetic performance several days after the end of the heat stress. Although the thermal-tolerant *C. nodosa* is likely to be more resistant and resilient to above-normal temperatures than *Z. marina*, it seems to be close to its thermal tolerance in Ria Formosa. Hence, the distribution of both species is likely to be negatively altered by more frequent and intense MHW events. Through the example of Ria Formosa, this study stresses the importance of seagrass conservation worldwide.

Yet, the resilience of *C. nodosa* to MHWs must be investigated on a longer time scale (e.g., after a more extended recovery period) to know whether such consequences are irreversible or if this species can recover entirely from the heatwave. The consequences of MHWs on *C. nodosa* might also depend on the characteristics the events (peak temperature, reoccurrence, duration of the event, time of the year…), as physiological responses can vary from positive to negative and at different time scales. The totality of physiological responses of *C. nodosa* to MHWs remain poorly known and difficult to assess with a few experiments simulating specific MHW events. Further investigation is yet to be made to precisely understand how this species copes with such events.

6. References

Alongi, D. M. (2018). Blue carbon: Coastal sequestration for climate change mitigation. Cham, Switzerland: Springer.

Andrade, J. P. (1985). Aspectos geomorfológicos, ecológicos e socioeconómicos da Ria Formosa (91 pp.). Faro: Universidade do Algarve.

Apel, K. & Hirt, H. (2004). Reactive oxygen species: metabolism, oxidative stress, and signal transduction. *Annual Review of Plant Biology,* **55**, 373–399. https://doi.org/10.1146/annurev.arplant.55.031903.141701

Arias-Ortiz, A., Serrano, O., Masqué, P., Lavery, P. S., Mueller, U., Kendrick, G. A., Rozaimi, M., Esteban, A., Fourqurean, J. W., Marbà, N., Mateo, M. A., Murray, K., Rule, M. and Duarte, C. M. (2018). A marine heatwave drives massive losses from the world's largest seagrass carbon stocks. *Nature Climate Change*, **8**(4), 338. https://doi.org/10.1038/s41558-018-0096-y

Bannister, T. T. (1979). Quantitative description of steady state, nutrient-saturated algal growth, including adaptation. *Limnology and Oceanography*, **24**(1), 76-96. https://doi.org/10.4319/lo.1979.24.1.0076

Bañolas, G., Fernández, S., Espino, F., Haroun, R. and Tuya, F. (2020). Evaluation of carbon sinks by the seagrass *Cymodocea nodosa* at an oceanic island: Spatial variation and economic valuation. *Ocean & Coastal Management*, **187**, 105112. https://doi.org/10.1016/j.ocecoaman.2020.105112

Banzon, V., Smith, T. M., Chin, T. M., Liu, C. and Hankins, W. (2016). A long-term record of blended satellite and in situ sea-surface temperature for climate monitoring, modelling and environmental studies. *Earth System Science Data*, **8**, 165–176. https://doi:10.5194/essd-8-165-2016

Beca-Carretero, P., Guihéneuf, F., Krause-Jensen, D. and Stengel, D. B. (2020). Seagrass fatty acid profiles as a sensitive indicator of climate settings across seasons and latitudes. *Marine Environmental Research*, **161**, 105075. https://doi.org/10.1016/j.marenvres.2020.105075

Beca-Carretero, P., Guihéneuf, F., Marín-Guirao, L., Bernardeau-Esteller, J., García-Muñoz, R., Stengel, D. B. and Ruiz, J. M. (2018). Effects of an experimental heat wave on fatty acid composition in two Mediterranean seagrass species. *Marine pollution bulletin*, **134**, 27-37. https://doi.org/10.1016/j.marpolbul.2017.12.057

Beca-Carretero, P., Olesen, B., Marbà, N. and Krause-Jensen, D. (2018). Response to experimental warming in northern eelgrass populations: comparison across a range of temperature adaptations. *Marine Ecology Progress Series,* **589**, 59–72. https://doi.org/10.3354/meps12439

Beer, S., Björk, M., Gademann, R. and Ralph, P. (2001). Measurements of photosynthetic rates in seagrasses. In *Global seagrass research methods* (pp. 183-198). Elsevier Science.

Bergmann, N., Winters, G., Rauch, G., Eizaguirre, C., Gu, J., Nelle, P., Fricke, B. and Reusch, T.B. (2010). Population-specificity of heat stress gene induction in northern and southern eelgrass *Zostera marina* populations under simulated global warming. *Molecular Ecology*, **19** (14), 2870–2883. https://doi.org/10.1111/j.1365-294X.2010.04731.x

Blandon, A., & Zu Ermgassen, P. S. (2014). Quantitative estimate of commercial fish enhancement by seagrass habitat in southern Australia. *Estuarine, Coastal and Shelf Science*, **141**, 1-8. https://doi.org/10.1016/j.ecss.2014.01.009

Booker, F. L., & Miller, J. E. (1998). Phenylpropanoid metabolism and phenolic composition of soybean [*Glycine max* (L.) Merr.] leaves following exposure to ozone. *Journal of Experimental Botany*, **49**(324), 1191-1202. https://doi.org/10.1093/jxb/49.324.1191

Boudouresque, C. F., Mayot, N. and Pergent, G. (2006). The outstanding traits of the functioning of the *Posidonia oceanica* seagrass ecosystem. *Biologie Marine Mediterranée*, **13**(4), 109-113.

Brodersen, K. E., Kühl, M., Nielsen, D. A., Pedersen, O., and Larkum, A. W. (2018). Rhizome, root/sediment interactions, aerenchyma and internal pressure changes in seagrasses. In *Seagrasses of Australia* (pp. 393-418). Springer, Cham. https://doi.org/10.1007/978-3-319-71354-0_13

Brodeur, R. D., Auth, T. D. and Phillips, A. J. (2019). Major shifts in pelagic micronekton and macrozooplankton community structure in an upwelling ecosystem related to an unprecedented marine heatwave. *Frontiers in Marine Science*, **6**, 212. https://doi.org/10.3389/fmars.2019.00212

Cabaço, S., Ferreira, Ó., and Santos, R. (2010). Population dynamics of the seagrass *Cymodocea nodosa* in Ria Formosa lagoon following inlet artificial relocation. *Estuarine, Coastal and Shelf Science*, **87**(4), 510-516. https://doi.org/10.1016/j.ecss.2010.02.002

Cabaço, S. & Santos, R. (2010). Reproduction of *Zostera marina* at the species southern distributional limit in the eastern Atlantic. *Marine Ecology*, **31**, 300–308. https://doi.org/10.1111/j.1439-0485.2009.00331.x

Cabaço, S. & Santos, R. (2014). Human-induced changes of the seagrass *Cymodocea nodosa* in Ria Formosa lagoon (Southern Portugal) after a decade. *Cahiers de Biologie Marine*, **55**, 101-108.

Carr, J., D'odorico, P., McGlathery, K. and Wiberg, P. L. (2010). Stability and bistability of seagrass ecosystems in shallow coastal lagoons: Role of feedbacks with sediment resuspension and light attenuation. *Journal of Geophysical Research: Biogeosciences*, **115**(G3). https://doi.org/10.1029/2009JG001103

Chalanika De Silva, H. C. & Asaeda, T. (2017). Effects of heat stress on growth, photosynthetic pigments, oxidative damage and competitive capacity of three submerged macrophytes. *Journal of Plant Interactions*, **12**(1), 228-236. https://doi.org/10.1080/17429145.2017.1322153

Collier, C. J., Ow, Y. X., Langlois, L., Uthicke, S., Johansson, C. L., O'Brien, K. R., Hrebien, V. and Adams, M. P. (2017). Optimum temperatures for net primary productivity of three tropical seagrass species. *Frontiers in Plant Science*, **8**, 1446. https://doi.org/10.3389/fpls.2017.01446

Costa, M. M., Silva, J., Barrote, I. and Santos, R. (2021). Heatwave Effects on the Photosynthesis and Antioxidant Activity of the Seagrass *Cymodocea nodosa* under Contrasting Light Regimes. *Oceans*, **2**(3), 448-460. https://doi.org/10.3390/oceans2030025

Cunha, A. H., Assis, J. F. and Serrão, E. A. (2014). Reprint of "Seagrasses in Portugal: A most endangered marine habitat". *Aquatic botany*, **115**, 3-13. https://doi.org/10.1016/j.aquabot.2011.08.007

Cunha, A. H. & Duarte, C. M. (2005). Population age structure and rhizome growth of *Cymodocea nodosa* in the Ria Formosa (southern Portugal). *Marine Biology*, **146**(5), 841-847. https://10.1007/s00227-004-1496-2

Cunha, A. H., Paulo, D. S., Sousa, I. and Serrão, E. (2013). The rediscovery of *Caulerpa prolifera* in Ria Formosa, Portugal, 60 years after the previous record. *Cahiers de biologie marine*, **54**(3), 359-364.

de los Santos, C. B., Krause-Jensen, D., Alcoverro, T., Marbà, N., Duarte, C. M., van Katwijk, M. M., Pérez, M., Romero, J., Sánchez-Lizaso, J. L., Roca, G. et al. (2019). Recent trend reversal for declining European seagrass meadows. *Nature Communications*, **10**, 3356. https://doi.org/10.1038/s41467-019-11340-4

Du, Z. & Bramlage, W. J. (1992). Modified thiobarbituric acid assay for measuring lipid oxidation in sugar-rich plant tissue extracts. *Journal of Agricultural and Food Chemistry*, **40**(9), 1566-1570.

Duarte, C. M. (2002). The future of seagrass meadows. *Environmental conservation*, **29**(2), 192-206. https://doi.org/10.1017/S0376892902000127

Duarte, C. M. & Krause-Jensen, D. (2017). Export from seagrass meadows contributes to marine carbon sequestration. *Frontiers in Marine Science*, **4**, 13. https://doi.org/10.3389/fmars.2017.00013

Duarte, C. M., Marbà, N., Gacia, E., Fourqurean, J. W., Beggins, J., Barrón, C. and Apostolaki, E. T. (2010). Seagrass community metabolism: Assessing the carbon sink capacity of seagrass meadows. *Global Biogeochemical Cycles*, **24**(4). https://doi.org/10.1029/2010GB003793

Duarte, C. M., Middelburg, J. J. and Caraco, N. (2005). Major role of marine vegetation on the oceanic carbon cycle. *Biogeosciences*, **2**(1), 1-8. https://doi.org/10.5194/bg-2-1-2005

Egea, L. G., Jiménez–Ramos, R., Hernández, I. and Brun, F. G. (2019). Effect of *In Situ* short–term temperature increase on carbon metabolism and dissolved organic carbon (DOC) fluxes in a community dominated by the seagrass *Cymodocea nodosa*. *PloS one*, **14**(1), e0210386. https://doi.org/10.1371/journal.pone.0210386

Egea, L. G., Jiménez-Ramos, R., Vergara, J. J., Hernández, I. and Brun, F. G. (2018). Interactive effect of temperature, acidification and ammonium enrichment on the seagrass *Cymodocea nodosa*. *Marine pollution bulletin*, **134**, 14-26. https://doi.org/10.1016/j.marpolbul.2018.02.029

Falcão, M. & Vale, C. (1990). Study of the Ria Formosa ecosystem: benthic nutrient remineralization and tidal variability of nutrients in the water. *Hydrobiologia*, **207**(1), 137–146.

Field, C. B., Barros, V., Stocker, T. F. and Dahe, Q. (Eds.). (2012). *Managing the risks of extreme events and disasters to advance climate change adaptation: special report of the intergovernmental panel on climate change (IPCC)*. Cambridge University Press.

Folin, O. & Ciocalteu, V. (1927). On tyrosine and tryptophane determinations in proteins. *Journal of biological chemistry*, **73**(2), 627-650.

Franssen, S. U., Gu, J., Bergmann, N., Winters, G., Klostermeier, U. C., Rosenstiel, P., Bornberg-Bauer, E. and Reusch, T. B. (2011). Transcriptomic resilience to global warming in the seagrass *Zostera marina*, a marine foundation species. *Proceedings of the National Academy of Sciences*, **108**(48), 19276-19281. https://doi.org/10.1073/pnas.1107680108

Franssen, S. U., Gu, J., Winters, G., Huylmans, A. K., Wienpahl, I., Sparwel, M., Coyer, J.A., Olsen, J.L., Reusch, T.B.H. and Bornberg-Bauer, E. (2014). Genome-wide transcriptomic responses of the seagrasses *Zostera marina* and *Nanozostera noltii* under a simulated heatwave confirm functional types. *Marine Genomics*, **15**, 65-73. https://doi.org/10.1016/j.margen.2014.03.004

Gao, Y., Jiang, Z., Du, M., Fang, J., Jiang, W. and Fang, J. (2019). Photosynthetic and metabolic responses of eelgrass *Zostera marina L*. to short-term high-temperature exposure. *Journal of Oceanology and Limnology*, **37**(1), 199-209. https://doi.org/10.1007/s00343-019-7319-6

Genevier, L. G., Jamil, T., Raitsos, D. E., Krokos, G. and Hoteit, I. (2019). Marine heatwaves reveal coral reef zones susceptible to bleaching in the Red Sea. *Global change biology*, **25**(7), 2338-2351. https://doi.org/10.1111/gcb.14652

George, R., Gullström, M., Mangora, M. M., Mtolera, M. S. and Björk, M. (2018). High midday temperature stress has stronger effects on biomass than on photosynthesis: a mesocosm experiment on four tropical seagrass species. *Ecology and Evolution*, **8**(9), 4508-4517. https://doi.org/10.1002/ece3.3952

Gibble, C., Duerr, R., Bodenstein, B., Lindquist, K., Lindsey, J., Beck, J., Henkel, L., Roletto, J., Harvey, J. and Kudela, R. (2018). Investigation of a largescale Common Murre (*Uria aalge*) mortality event in California, USA, in 2015. *Journal of wildlife diseases*, **54**(3), 569-574. https://doi.org/10.7589/2017-07-179

Gillespie, K. M., Chae, J. M. and Ainsworth, E. A. (2007). Rapid measurement of total antioxidant capacity in plants. *Nature protocols*, **2**(4), 867-870. https://doi.org/10.1038/nprot.2007.100

Green, E. P. & Short, F. T. (2003). *World atlas of seagrasses*. University of California Press.

Gu, J., Weber, K., Klemp, E., Winters, G., Franssen, S. U., Wienpahl, I., Huylmans, A., Zecher, K., Reusch, T.B.H., Bornberg-Bauer, E. and Weber, A. P. (2012). Identifying core features of adaptive metabolic mechanisms for chronic heat stress attenuation contributing to systems robustness. *Integrative Biology*, **4**(5), 480-493. https://doi.org/10.1039/c2ib00109h

Guerrero-Meseguer, L., Veiga, P., Sampaio, L. and Rubal, M. (2021). Resurgence of *Zostera marina* in the Ria de Aveiro lagoon, Portugal. *Aquatic Botany*, **169**, 103338. https://doi.org/10.1016/j.aquabot.2020.103338

Guimarães, M. H. M., Cunha, A. H., Nzinga, R. L. and Marques, J. F. (2012). The distribution of seagrass (*Zostera noltii*) in the Ria Formosa lagoon system and the implications of clam farming on its conservation. *Journal for Nature Conservation*, **20**(1), 30-40. https://doi.org/10.1016/j.jnc.2011.07.005

Guirguis, K., Gershunov, A., Tardy, A. and Basu, R. (2014). The impact of recent heat waves on human health in California. *Journal of Applied Meteorology and Climatology,* **53**(1), 3-19. https://doi.org/10.1175/JAMC-D-13-0130.1

Heath, R. L. & Packer, L. (1968). Photoperoxidation in isolated chloroplasts: I. Kinetics and stoichiometry of fatty acid peroxidation. *Archives of biochemistry and biophysics*, **125**(1), 189-198. https://doi.org/10.1016/0003-9861(68)90654-1

Henley, W.J. (1993). Measurement and interpretation of photosynthetic light-response curves in algae in the context of photoinhibiotion and diel changes. *Journal of Phycology* **29**: 729–739. https://doi.org/10.1111/j.0022-3646.1993.00729.x

Hobday, A. J., Oliver, E. C., Gupta, A. S., Benthuysen, J. A., Burrows, M. T., Donat, M. G., Holbrook, N. J., Moore, P. J., Thomsen, M. S., Wernberg, T. and Smale, D. A. (2018). Categorizing and naming marine heatwaves. *Oceanography,* **31**(2), 162-173. https://doi.org/10.5670/oceanog.2018.205

Hobday, A.J., Alexander, L.V., Perkins, S.E., Smale, D.A., Straub, S.C., Oliver, E.C., Benthuysen, J.A., Burrows, M.T., Donat, M.G., Feng, M. and Holbrook, N.J. (2016). A hierarchical approach to defining marine heatwaves. *Progress in Oceanography*, **141**, pp.227-238. https://doi.org/10.1016/j.pocean.2015.12.014

Hodges, D. M., DeLong, J. M., Forney, C. F. and Prange, R. K. (1999). Improving the thiobarbituric acid-reactive-substances assay for estimating lipid peroxidation in plant tissues containing anthocyanin and other interfering compounds. *Planta*, **207**(4), 604-611. https://doi.org/10.1007/s004250050524

Holbrook, N. J., Scannell, H. A., Gupta, A. S., Benthuysen, J. A., Feng, M., Oliver, E. C., Alexamder L.V., Burrows, M.T., Donat, M.G., Hobday, A.J., Moore, P. J., Perkins-Kirkpatrick, S.E., Smale, D.A., Straub, S.C. and Wernberg, T. (2019). A global assessment of marine heatwaves and their drivers. *Nature communications*, **10**(1), 1-13. https://doi.org/10.1038/s41467-019-10206-z

Holbrook, N.J., Sen Gupta, A., Oliver, E.C.J., Hobday, A.J., Benthuysen, J.A., Scannel, H.A., Smale D.A. and Wernberg, T. (2020). Keeping pace with marine heatwaves. *Nature Review Earth Environnment,* **1**, 482–493. https://doi.org/10.1038/s43017-020-0068-4

Huang, B., Liu, C., Banzon, V., Freeman, E., Graham, G., Hankins, B., Smith, T. and Zhang, H.-M. (2020). Improvements of the Daily Optimum Interpolation Sea Surface Temperature (DOISST) Version 2.1, *Journal of Climate*, **34**, 2923-2939. https://doi.org/10.1175/JCLI-D-20-0166.1

Huang, D., Ou, B., Hampsch-Woodill, M., Flanagan, J.A. and Prior, R.L. (2002) High-Throughput Assay of Oxygen Radical Absorbance Capacity (ORAC) Using a Multichannel Liquid Handling System Coupled with a Microplate Fluorescence Reader in 96-Well Format. *Journal of Agricultural and Food Chemistry*, **50**, 4437-4444. https://doi.org/10.1021/jf0201529

Hughes, T. P., Kerry, J. T., Baird, A. H., Connolly, S. R., Dietzel, A., Eakin, C. M., Heron, S. F., Hoey, A. S., Hoogenboom, M. O., Liu, G., McWilliam, M. J., Pears, R. J., Pratchett, M. S., Skirving, W. J., Stella, J. S. and Torda, G. (2018). Global warming transforms coral reef assemblages. *Nature*, **556**(7702), 492-496. https://doi.org/10.1038/s41586-018-0041-2

Instituto Hidrográfico (1986). Marés 81/82 Ria de Faro. Estudo das marés de oito estacões da Ria de Faro (13 pp.). Lisbon: Instituto Hidrográfico, (Rel.FT-MC-4/86).

IPCC, 2019: IPCC Special Report on the Ocean and Cryosphere in a Changing Climate [Pörtner, H.-O. Roberts, D.C., Masson-Delmotte, V., Zhai, P., Tignor, M., Poloczanska, E., Mintenbeck, K., Alegría, A., Nicolai, M., Okem, A., Petzold, J., Rama, B. and Weyer, N.M.]. In press.

Jassby, A. D. & Platt, T. (1976). Mathematical formulation of the relationship between photosynthesis and light for phytoplankton. *Limnology and oceanography*, **21**(4), 540-547. https://doi.org/10.4319/lo.1976.21.4.0540

Jueterbock, A., Boström, C., Coyer, J. A., Olsen, J. L., Kopp, M., Dhanasiri, A. K., Smolina, I., Arnaud-Haond, S., Van de Peer, Y. and Hoarau, G. (2020). The seagrass methylome is associated with variation in photosynthetic performance among clonal shoots. *Frontiers in plant science*, **11**, 1387. https://doi.org/10.3389/fpls.2020.571646

Kennedy, H., Beggins, J., Duarte, C. M., Fourqurean, J. W., Holmer, M., Marbà, N. and Middelburg, J. J. (2010). Seagrass sediments as a global carbon sink: Isotopic constraints. *Global Biogeochemical Cycles*, **24**(4). https://doi.org/10.1029/2010GB003848

Kim, M., Qin, L. Z., Kim, S. H., Song, H. J., Kim, Y. K. and Lee, K. S. (2020). Influence of water temperature anomalies on the growth of Zostera marina plants held under high and low irradiance levels. *Estuaries and Coasts*, **43**(3), 463-476. https://doi.org/10.1007/s12237-019-00578-2

Le Nohaïc, M., Ross, C. L., Cornwall, C. E., Comeau, S., Lowe, R., McCulloch, M. T. and Schoepf, V. (2017). Marine heatwave causes unprecedented regional mass bleaching of thermally resistant corals in northwestern Australia. *Scientific Reports*, **7**(1), 1-11. https://doi.org/10.1038/s41598-017-14794-y

Lee, K. S., Park, S. R. and Kim, Y. K. (2007). Effects of irradiance, temperature, and nutrients on growth dynamics of seagrasses: a review. *Journal of Experimental Marine Biology and Ecology*, **350**(1-2), 144-175. https://doi.org/10.1016/j.jembe.2007.06.016

Leggat, W. P., Camp, E. F., Suggett, D. J., Heron, S. F., Fordyce, A. J., Gardner, S., Deakin, L., Turner, M., Beeching, L. J., Kuzhiumparambil, U., Eakin, C. M. and Ainsworth, T. D. (2019). Rapid coral decay is associated with marine heatwave mortality events on reefs. *Current Biology*, **29**(16), 2723-2730. https://doi.org/10.1016/j.cub.2019.06.077

Lüning, K. (1990). Seaweeds. Their environment, biogeography, and ecophysiology. Wiley-Interscience, New York.

Marbà, N., Krause-Jensen, D., Masqué, P. and Duarte, C. M. (2018). Expanding Greenland seagrass meadows contribute new sediment carbon sinks. *Scientific reports*, **8**(1), 1-8. https://doi.org/10.1038/s41598-018-32249-w

Marín-Guirao, L., Bernardeau-Esteller, J., García-Muñoz, R., Ramos, A., Ontoria, Y., Romero, J., Pérez, M., Ruiz, J. M. and Procaccini, G. (2018). Carbon economy of Mediterranean seagrasses in response to thermal stress. *Marine pollution bulletin*, **135**, 617-629. https://doi.org/10.1016/j.marpolbul.2018.07.050

Marín-Guirao, L., Ruiz, J. M., Dattolo, E., Garcia-Munoz, R. and Procaccini, G. (2016). Physiological and molecular evidence of differential short-term heat tolerance in Mediterranean seagrasses. *Scientific reports*, **6**(1), 1-13. https://doi.org/10.1038/srep28615

Massa, S. I., Arnaud-Haond, S., Pearson, G. A. and Serrão, E. A. (2009). Temperature tolerance and survival of intertidal populations of the seagrass *Zostera noltii* (Hornemann) in Southern Europe (Ria Formosa, Portugal). *Hydrobiologia*, **619**, 195–201. https://doi.org/10.1007/s10750-008-9609-4

Maxwell, K. & Johnson, G.N (2000). Chlorophyll fluorescence—A practical guide. *Journal of experimental botany*, **51**, 659–668. https://doi.org/10.1093/jexbot/51.345.659

Mehler, A.H. (1951). Studies on reactions of illuminated chloroplasts. II Stimulation and inhibition of the reaction with molecular oxygen. *Archives of Biochemistry and Biophysics*, **34**(2), 339–51. https://doi.org/10.1016/0003-9861(51)90012-4

Moreno-Marín, F., Brun, F. G. and Pedersen, M. F. (2018). Additive response to multiple environmental stressors in the seagrass *Zostera marina* L. *Limnology and Oceanography*, **63**(4), 1528-1544. https://doi.org/10.1002/lno.10789

Nejrup, L. B. & Pedersen, M. F. (2008). Effects of salinity and water temperature on the ecological performance of *Zostera marina*. *Aquatic Botany*, ***88***(3), 239-246. https://doi.org/10.1016/j.aquabot.2007.10.006

Newton, A. & Mudge, S. M. (2003). Temperature and salinity regimes in a shallow, mesotidal lagoon, the Ria Formosa, Portugal. Estuarine, Coastal and Shelf Science, **57**(1–2), 73-85. https://doi.org/10.1016/S0272-7714(02)00332-3

Oliver, E. C. J., Donat, M.G., Burrows, M.T., Moore, P.J., Smale, D.A., Alexander, L.V., Benthuysen, J.A., Feng, M., Gupta, A.S., Hobday, A. J., Holbrook, N.J., Perkins-Kirkpatrick, S.E., Scannell, H.A., Straub, S.C. and Wernberg, T. (2018). Longer and more frequent marine heatwaves over the past century. *Nature Communications*, **9**, 1324. https://doi.org/10.1038/s41467-018-03732-9

Oliver, E. C., Burrows, M. T., Donat, M. G., Sen Gupta, A., Alexander, L. V., Perkins-Kirkpatrick, S. E., Benthuysen, J.A., Hobday, A.J., Holbrook, N.J., Moore, P.J., Thomsen, M.S., Wernberg, T. and Smale, D.A. (2019). Projected marine heatwaves in the 21st century and the potential for ecological impact. *Frontiers in Marine Science*, **6**, 734. https://doi.org/10.3389/fmars.2019.00734

Olsen, Y. S., Sánchez-Camacho, M., Marbà, N. and Duarte, C. M. (2012). Mediterranean seagrass growth and demography responses to experimental warming. *Estuaries and coasts*, **35**(5), 1205-1213. https://doi.org/10.1007/s12237-012-9521-z

Orth, R. J., Carruthers, T. J., Dennison, W. C., Duarte, C. M., Fourqurean, J. W., Heck, K. L., Hughes, A. R., Kendrick, G. A., Kenworthy, W. J., Olyarnik, S., Short, F. T., Waycott, M. and Williams, S. L. (2006). A global crisis for seagrass ecosystems. *Bioscience*, **56**(12), 987-996. https://doi.org/10.1641/0006-3568(2006)56[987:AGCFSE]2.0.CO;2

Pérez, M. & Romero, J. (1992). Photosynthetic response to light and temperature of the seagrass *Cymodocea nodosa* and the prediction of its seasonality. *Aquatic Botany*, **43**(1), 51-62. https://doi.org/10.1016/0304-3770(92)90013-9

Pérez, M., Duarte, C. M., Romero, J., Sand-Jensen, K. and Alcoverro, T. (1994). Growth plasticity in *Cymodocea nodosa* stands: the importance of nutrient supply. *Aquatic Botany*, **47**(3–4), 249–264. https://doi.org/10.1016/0304-3770(94)90056-6

Perkins-Kirkpatrick, S. E., King, A. D., Cougnon, E. A., Holbrook, N. J., Grose, M. R., Oliver, E. C. J., Lewis, S.C. and Pourasghar, F. (2019). The role of natural variability and anthropogenic climate change in the 2017/18 Tasman Sea marine heatwave. *Bulletin of the American Meteorological Society*, **100**(1), S105-S110. https://doi.org/10.1175/BAMS-D-18-0116.1

Prior, R. L., Wu, X. and Schaich, K. (2005). Standardized methods for the determination of antioxidant capacity and phenolics in foods and dietary supplements. *Journal of agricultural and food chemistry*, **53**(10), 4290-4302. https://doi.org/10.1021/jf0502698

Qin, L. Z., Kim, S. H., Song, H. J., Suonan, Z., Kim, H., Kwon, O. and Lee, K. S. (2020). Influence of regional water temperature variability on the flowering phenology and sexual reproduction of the seagrass *Zostera marina* in Korean coastal waters. *Estuaries and Coasts*, **43**(3), 449-462. https://doi.org/10.1007/s12237-019-00569-3

R Core Team (2014). R: A language and environment for statistical computing. R Foundation for Statistical Computing, Vienna, Austria. http://www.R-project.org/

Rasband, W.S., ImageJ, U. S. National Institutes of Health, Bethesda, Maryland, USA, 1997-2018. https://imagej.nih.gov/ij/

Re, R., Pellegrini, N., Proteggente, A., Pannala, A., Yang, M. and Rice-Evans, C. (1999). Antioxidant activity applying an improved ABTS radical cation decolorization assay. *Free radical biology and medicine*, **26**(9-10), 1231-1237. https://doi.org/10.1016/S0891-5849(98)00315-3

Repolho, T., Duarte, B., Dionísio, G., Paula, J. R., Lopes, A. R., Rosa, I. C., Grilo, T. F., Caçador, I., Calado, R. and Rosa, R. (2017). Seagrass ecophysiological performance under ocean warming and acidification. *Scientific Reports,* **7**, 41443. https://doi.org/10.1038/srep41443

Reynolds, R. W., Smith, T. M., Liu, C., Chelton, D. B., Casey, K. S. and Schlax, M. G. (2007). Daily high-resolution-blended analyses for sea surface temperature. *Journal of Climate*, **20**, 5473–5496. https://doi.org/10.1175/JCLI-D-14-00293.1

Saha, M., Barboza, F. R., Somerfield, P. J., Al-Janabi, B., Beck, M., Brakel, J. et al. (2020). Response of foundation macrophytes to near-natural simulated marine heatwaves. *Global change biology*, **26**(2), 417-430. https://doi.org/10.1111/gcb.14801

Savva, I., Bennett, S., Roca, G., Jordà, G. and Marbà, N. (2018). Thermal tolerance of Mediterranean marine macrophytes: Vulnerability to global warming. *Ecology and Evolution*, **8**(23), 12032-12043. https://doi.org/10.1002/ece3.4663

Schlegel, R. W. (2020). Marine Heatwave Tracker. http://www.marineheatwaves.org/tracker, https://doi.org/10.5281/zenodo.3787872

Schubert, N., Freitas, C., Silva, A., Costa, M. M., Barrote, I., Horta, P. A., Rodrigues, A. C., Santos, R. and Silva, J. (2018). Photoacclimation strategies in northeastern Atlantic seagrasses: Integrating responses across plant organizational levels. *Scientific reports*, **8**(1), 1-14. https://doi.org/10.1038/s41598-018-33259-4

Shahidi, F. & Zhong, Y. (2015). Measurement of antioxidant activity. *Journal of functional foods*, **18**, 757-781. https://doi.org/10.1016/j.jff.2015.01.047

Silva, J. & Santos, R. (2004). Can chlorophyll fluorescence be used to estimate photosynthetic production in the seagrass *Zostera noltii*? *Journal of Experimental Marine Biology and Ecology*, **307**(2), 207-216. https://doi.org/10.1016/j.jembe.2004.02.009

Silva, J., Barrote, I., Costa, M. M., Albano, S. and Santos, R. (2013). Physiological responses of *Zostera marina* and *Cymodocea nodosa* to light-limitation stress. *PloS one*, **8**(11), e81058. https://doi.org/10.1371/journal.pone.0081058

Smale, D. A., Wernberg, T., Oliver, E. C., Thomsen, M., Harvey, B. P., Straub, S. C., Burrows, M. T., Alexander, L. V., Benthuysen, J. A., Donat, M. G., Feng, M., Hobday, A. J., Holbrook, N. J., Perkins-Kirkpatrick, S. E., Scannell, H. A., Gupta, A. S., Payne, B. L. and Moore, P. J. (2019). Marine heatwaves threaten global biodiversity and the provision of ecosystem services. *Nature Climate Change*, **9**(4), 306-312. https://doi.org/10.1038/s41558-019-0412-1

Smith, E. L. (1936). Photosynthesis in relation to light and carbon dioxide. *Proceedings of the National Academy of Sciences of the United States of America*, **22**(8), 504. https://dx.doi.org/10.1073%2Fpnas.22.8.504

Talling, J. F. (1957). Photosynthetic characteristics of some freshwater plankton diatoms in relation to underwater radiation. *New Phytologist*, **56**(1), 29-50. https://doi.org/10.1111/j.1469-8137.1957.tb07447.x

Taulavuori, E., Hellström, E. K., Taulavuori, K. and Laine, K. (2001). Comparison of two methods used to analyse lipid peroxidation from *Vaccinium myrtillus* (L.) during snow removal, reacclimation and cold acclimation. *Journal of Experimental Botany*, **52**(365), 2375-2380. https://doi.org/10.1093/jexbot/52.365.2375

Tutar, O., Marín-Guirao, L., Ruiz, J. M. and Procaccini, G. (2017). Antioxidant response to heat stress in seagrasses. A gene expression study. *Marine environmental research*, **132**, 94-102. https://doi.org/10.1016/j.marenvres.2017.10.011

Waycott, M., Duarte, C. M., Carruthers, T. J., Orth, R. J., Dennison, W. C., Olyarnik, S., Calladine, A., Fourqurean, J. W., Heck Jr., K. L., Hughes, A. R., Kendrick, G. A., Kenworthy, W. J., Short, F.T. and Williams, S. L. (2009). Accelerating loss of seagrasses across the globe threatens coastal ecosystems. *Proceedings of the national academy of sciences*, **106**(30), 12377-12381. https://doi.org/10.1073/pnas.0905620106

Winters, G., Nelle, P., Fricke, B., Rauch, G. and Reusch, T. B. H. (2011) Effects of a simulated heat wave on photophysiology and gene expression of high- and low-latitude populations of *Zostera marina*. *Marine Ecology Progress Series*, **435**, 83-95. https://doi.org/10.3354/meps09213